Journal of African Earth Sciences 138 (2018) 348–366

Contents lists available at ScienceDirect

Journal of African Earth Sciences

journal homepage: www.elsevier.com/locate/jafrearsci

Hydro-geochemical characterizations of a platinum group element groundwater system in Africa

D. Pacome Ahokpossi*, Abdon Atangana, P. Danie Vermeulen

Institute for Groundwater Studies, Faculty of Natural and Agricultural Science, University of Free State, 9300 Bloemfontein, South Africa

ARTICLE INFO

Article history:
Received 20 March 2017
Received in revised form
20 November 2017
Accepted 22 November 2017
Available online 24 November 2017

Keywords:
Acid mine drainage
Pyrrhotite oxidation
Acid buffering
Serpentinite
Bushveld
Groundwater quality
Hydro-geochemical processes

ABSTRACT

Water is a scarce resource in the drylands of Africa and the Middle East and the identification of risks to aquifers is an important endeavor. There is a common and erroneous belief that only gold and coal deposits in Southern Africa are associated with acid-generating minerals. The study highlights the application the tools of geochemical analysis can reveal the classes of chemical reactions leading to the evolution of a shallow aquifer in an arid zone with active mining of sulfidic ore taking place.

The prevailing hydro-geochemical processes were assessed at an open cast platinum mine. Major conclusions relate to the Acid Mine Drainage buffering within fractured aquifer system associated with the platinum deposit. The oxidation of pyrrhotite from in situ sources is the major contributing factor towards AMD formation. Neutralization of acid in the groundwater system has solved the pH problem but introduced a salinity problem.

1. Introduction

Water is a scarce resource in the drylands of Africa and the Middle East and the identification of risks to aquifers is an important endeavor. The impact of acid mine drainage (AMD) on groundwater resource is one of the worse environmental concern associated with mining (Bell et al., 2001; Vermeulen and Usher, 2009).

The mining industry forms the backbone of the South African Economy. According to the Mineral Commodity Summaries (2015), South Africa is the world's largest producer of chrome, manganese, platinum, vanadium and vermiculite; and the second largest producer of ilmenite, palladium, rutile and zirconium. The country is also one of the largest coal exporters.

There is a common and erroneous belief that only gold and coal deposits in Southern Africa are associated with acid-generating minerals. This results in few investigations of the AMD potential of mining of Magmatic Sulfide Deposits in Bushveld Complex. The Platreef (Northern limb ore deposit in the BC) is known for its feldspathic pyroxenite-norite hosting one of the world class magnetic-type nickel, copper and platinum ground element (Kinnaird and McDonald, 2005). Since mid to late 1920's, the Plaatreef has become a site of platinum prospecting and mining (Buchanan, 1988).

In the process of AMD, a number of hydro-geochemical processes occur. Some of these processes are: acid neutralization/buffering, chemical precipitation, attenuation or dissolution of metals (Blowes et al., 1994). A sound hydro-geochemical conceptual model based on the site geology, hydrogeology, and mineralogy, is necessary for investigating the groundwater quality characteristics. One also needs to assess (test) the validity of each hypothetically conceived hydro-chemical reaction based on measured data.

The study aims to investigate the hydro-geochemical processes within the catchment and how they directly impact overall groundwater quality. It highlights the application of (bivariate) scatter plots, and other diagnostic plots as complimentary tools to analyze the groundwater chemistry data collected in a typical Platinum Group Element groundwater system. It specifically uses groundwater monitoring data from an open cast platinum mine to describe different hydro-geochemical process which prevail in the monitored groundwater system.

2. Description of the study area

The study area is located north-west of Mokopane town

* Corresponding author.
E-mail address: ahokposso@yahoo.fr (D.P. Ahokpossi).

https://doi.org/10.1016/j.jafrearsci.2017.11.032
1464-343X/

(approximately 30 km) within Mogalakwena Municipal Area, which forms part of the Waterberg District Municipality of the Limpopo Province, in South Africa (Fig. 1). Multiple open pit mines are operated by various mining companies. The area falls in catchment A61G which is located in the Limpopo Water Management Area, and is mainly drained by the Mogalkwena River toward the North. This area is used for a more general hypothesis for Platinum Group Element groundwater system in Africa.

The area normally receives up to 860 mm of rain per year. Most rainfall occurs during summer in the form of afternoon thunderstorms (Bye and Bell, 2001; Holland, 2011).

2.1. Soils and unsaturated zone

Based on existing borehole logs, and field observations, the top soil of the area consists mostly of clay and sand of multiple colors (whitish, blackish, brown). This soil has developed as residual soil from either the igneous or sedimentary rocks. This soil may extend to 3.0 m below ground level (mbgl), but is also absent at some places. The soils are classified as follows (Soil Classification Working Group, 1991; Fey, 2010).

- Sandy, loamy soils are found on the flatter areas (Hutton and Short-lands forms);
- At the Hilly area, shallower rocky soils (Mispha forms) are generally dominant;
- And the clay (sandy clay) soils (Arcadia form) are associated with depressions.

2.2. Hydro-stratigraphic units, types, and thicknesses

The subsurface geology (up to 180.0 mbgl) is characterized by a well-developed igneous layering of Gabbro-Norite (Rustenburg layered Suit, Bushveld Complex), Granite (Utrecht, Mashashane Suit), Pyroxinite, and Gneiss (and Goudplaats-Hout River Suit). These rocks form the hangingwall and the footwall of a platiniferous horizon, known as the Platreef. It has an economic platinum group element mineralization within a sulfide-bearing pyroxenite body. The strike length of the Platreef approximates between 35 km and 40 km (Viljoen and Schürmann, 1998; Manyeruke et al., 2005). The Platreef varies in thickness, with a maximum thickness of 400 m occurring in the south, thinning to less than 50.00 m in the north (Manyeruke et al., 2005). The thickness of the Platreef at Sandsloot ranges from 70.00 to 200.00 m (Bye and Bell, 2001). Rocks in these zones include cordierite spinel hornfels, clinopyroxenites, calcsilicates and graphite-bearing serpentinites, serpentinized peridotites and pyroxenites. Between Tweefontein and Sandsloot farms, a dolomite formation (of the Transvaal Super Group) known locally as the "dolomite tongue" thins the Platreef. At the farm Townlands, the Platreef consists of three packages of medium grained gabbronorite and, feldspathic pyroxenite, separated by hornfels interlayers, with a total thickness of approximately 150.00 m (Manyeruke et al., 2005). These igneous formations are disturbed by dolerite dykes of variable sizes, as well as by faults.

Depths to water-strike were analyzed from the drilling log of 45 existing boreholes. The depths to first water-strike are normally distributed. 85% of boreholes encountered water before a depth of

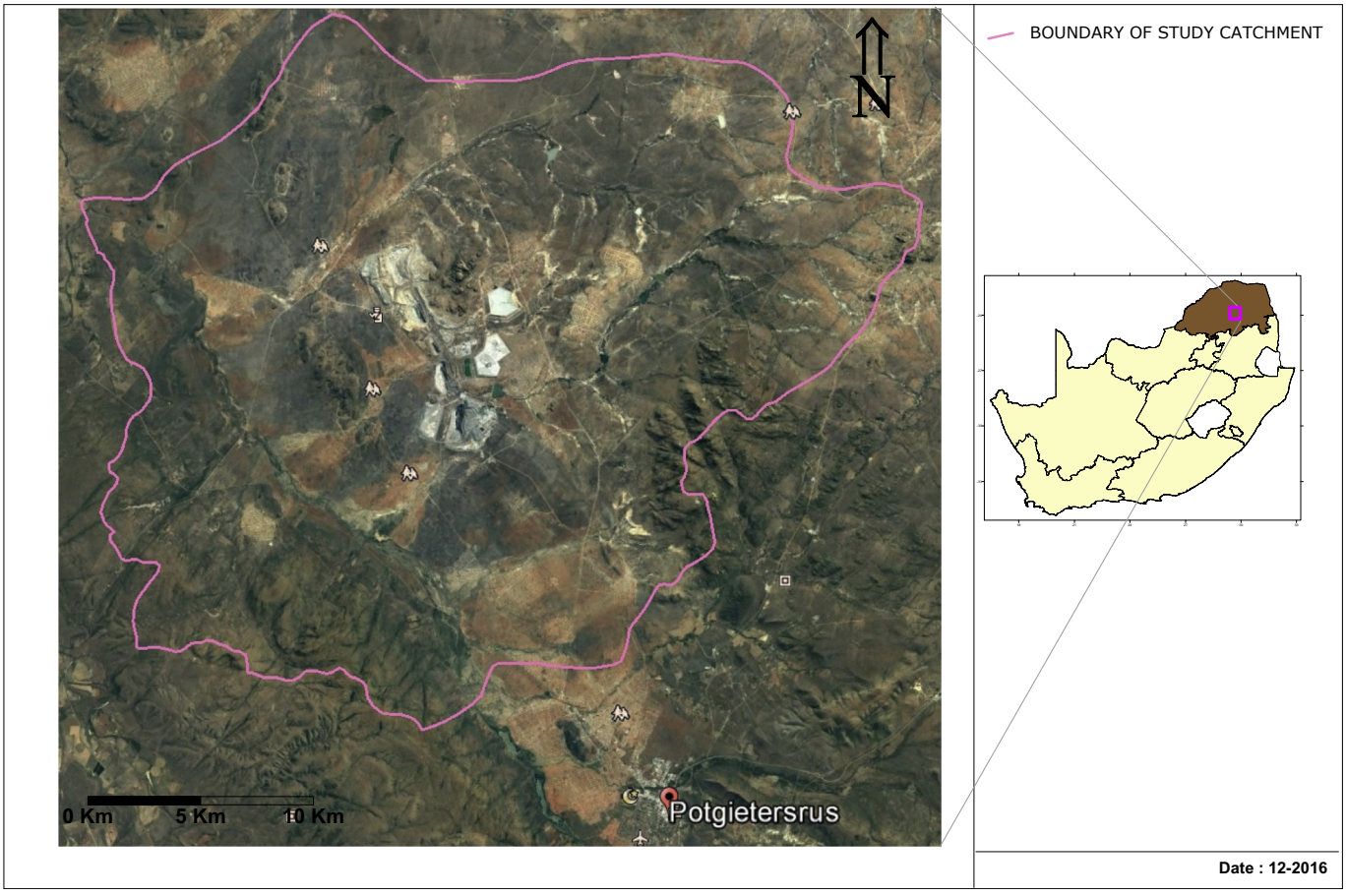

Fig. 1. Location of the study area.

25.00 m in the study area. The local average depth of weathering is 24.50 mbgl, with 88% of the recorded depth of weathering less than 35.00 mbgl. This typical distribution of the weathering contrasts to the general average depth of weathering/fracturing of 45.00 mbgl in the Limpopo Plateau Holland (2011).

From a hydro-geochemical point of view the only dominant important geological entities are: (1) Alluvial deposits; (2) Shallow weathered aquifer system; and (3) Shallow and Deeper Localized fracture aquifer system.

The recorded depths to groundwater levels from available borehole information show an approximately log-normal distribution (Fig. 2). The highest frequency (modes) between 5 and 15.0 mbgl and more than 95% of groundwater levels shallower than 20.00 mbgl. Such measured water levels result from the hydraulic heads equilibrium between both weathered and fractured aquifers.

Fig. 3 shows the location of the boreholes as recorded during different studies in the catchments (Hydrocensus, GRIP, Monitoring, etc. …). In the study area the groundwater is for multiple purpose, mainly for domestic, agricultural (Irrigation and cattle farming), and mining purposes. Such a multiple dependency on groundwater is often the case in Africa and Middle-East, and it is very important to safeguard the resource.

2.2.1. Alluvial aquifers

The majority of the alluvial deposits occur in the immediate vicinity of the rivers/streams/surface water drainage. Geological maps, and field observations, reveal that substantial deposits of alluvium occur along the major surface drainage course of the quaternary catchment: Mogalakwena River. The shallow alluvial aquifers may also be recharged along sections of this river, depending on the interactions between the two resources. The alluvial deposits typically consist of red or sandy clay (calcified in places) which overlies sand, gravel and pebbles. Sustainable yields from boreholes drilled into this aquifer vary between 0.50 ℓ/s and 9.00 ℓ/s (Holland, 2011).

2.2.2. Shallow weathered aquifer

The top soil is generally underlain by a sedimentary layer which may extend up to 9.00 m below ground level, with an average thickness of 3.00 m. This thin sedimentary layer forms the roof of the weathered/fractured igneous rocks and could be considered to be part of the shallow weathered aquifer. One of the previous models developed for the catchment considers this type of sedimentary layer as a sandy aquifer. However, the limited average thickness (less than 8.00 m) of such a layer, and the saturated level (depth to groundwater levels) of the aquifer, do not suggest a well-developed separate sandy aquifer, but rather, point to perched water tables within the weathered/fractured aquifer.

A proxy for the depth to bottom of weathering/fracturing zone (to fresh bedrock) was estimated by combining (weathering and fractures) dataset from fifty boreholes of the catchment. The top of the weathering and fracturing in the igneous rocks ranges between 1.00 and 23.00 mbgl, with an average of 6.50 mbgl. Weathering zones in the igneous rocks have an average thickness of 20.00 and occurred up to 50.00 mbgl. Fractures occur from 3.00 mgbl up to 75.00 mbgl. However, most of the fractures occur in the shallow weathering zone at depths between 10.00 and 40.00 mbgl (Fig. 4).

This aquifer is unconfined to semi-confined and is recharged by rainfall (Rian et al., 2009). Evidence of this is provided by the correlation between groundwater level elevation and topography (Fig. 5) as demonstrated by Henk and Sherry (2005).

The shallow weathered aquifer is comprised of low permeable rock material. The regional groundwater gradient is predominantly toward the Mogalakwena River, following the topography.

2.2.3. Deeper fractured aquifer

A deeper fractured rock aquifer is formed by fractured rocks of the Goudplaats-Hout River Gneiss Suit, Granites of the Mashashane Suit and Mashashane Suit. The predominant fracturing is linked to tectonic movements that took place during intrusions. There is insufficient information available to confirm the exact thickness of the deeper fractured aquifer.

The deeper fractured aquifer is expected to be unconfined to semi-confined, as available geological logs in the area did not show any impermeable layer between the Shallow weathered and the deeper aquifer systems.

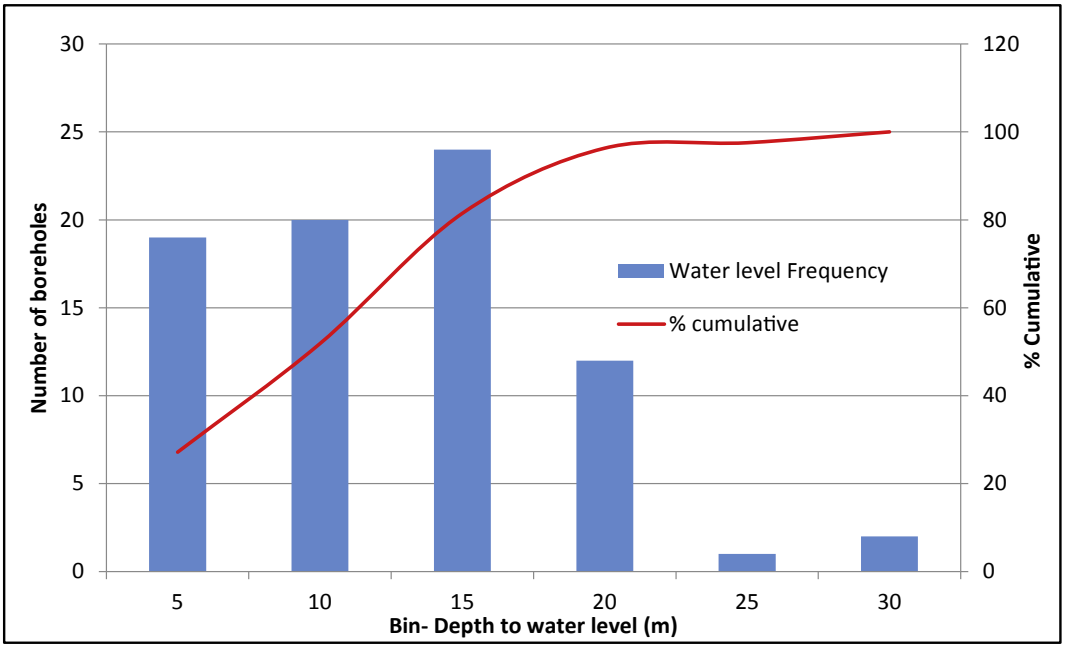

Fig. 2. Depth to groundwater levels frequency (Hydrocensus).

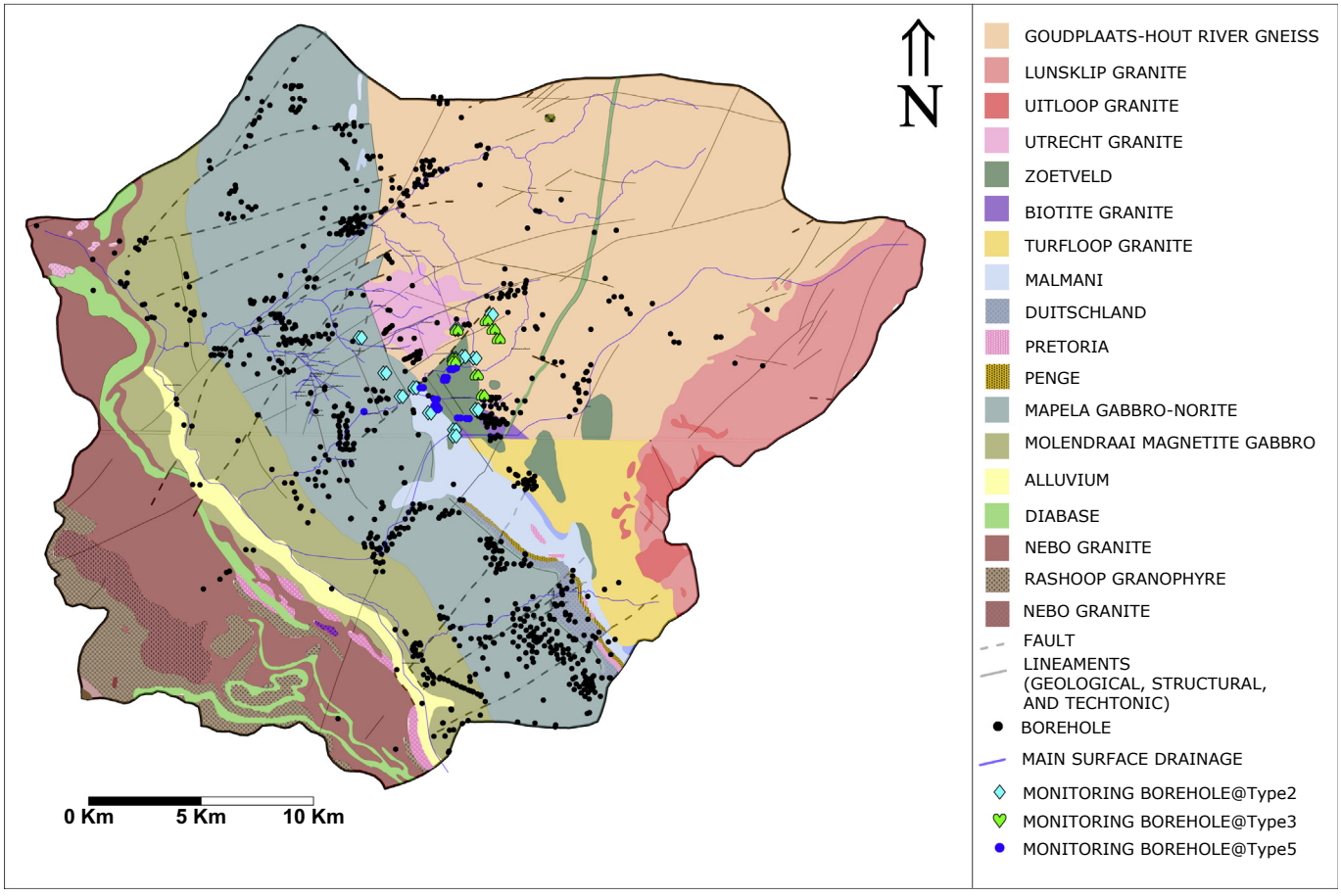

Fig. 3. Geology and locations of recorded boreholes in the catchment.

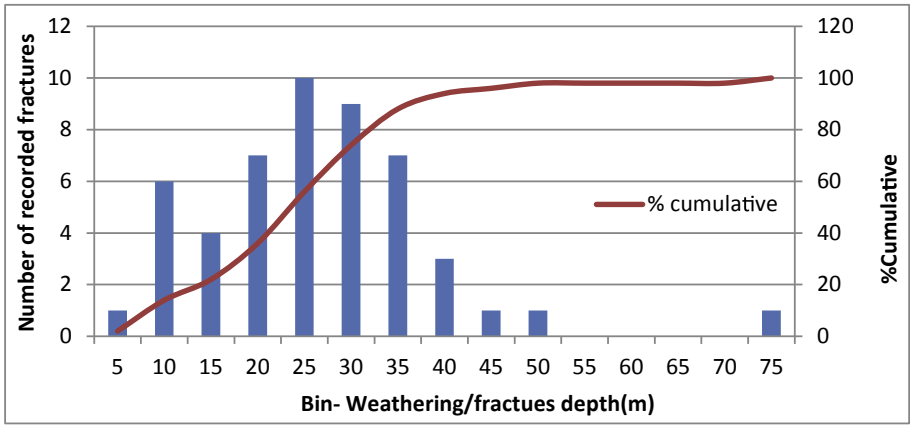

Fig. 4. Depth to first weathering bottom frequency (Boreholes logs).

3. Data collection and laboratory analysis

Groundwater chemistry data was obtained from Spot sampling (Hydrocensus) completed in March 2014 (from the 3rd to the 14th) over the entire quaternary catchment, and also from a monitoring period (Periodic sample) which extended over four years (2011–2014). The data was collected as part of a water resource protection and waste management program for a Mine in the catchment. The locations of the monitoring boreholes are shown in Fig. 3.

3.1. Groundwater sampling

Samples were collected according to the U.S. Environmental Protection Agency's (USEPA) low-flow sampling protocol (U.S. Environmental Protection Agency, 1996). Groundwater was

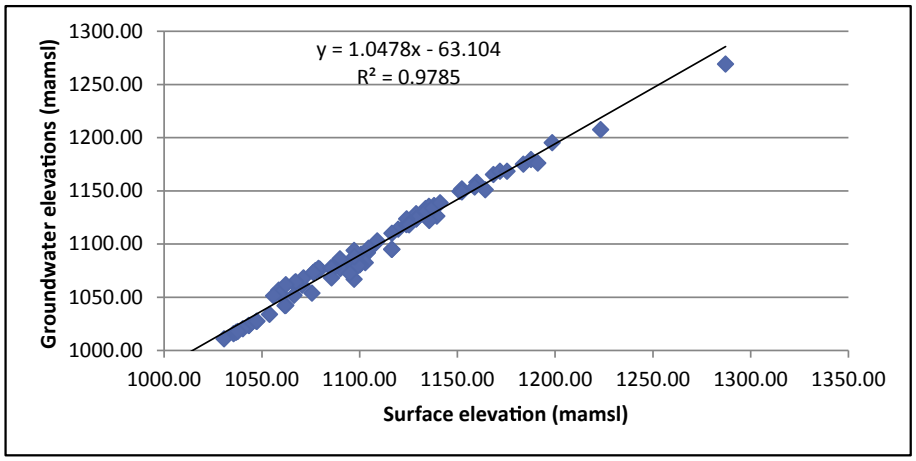

Fig. 5. Surface elevation correlation to groundwater elevations.

sampled from designated monitoring boreholes, after purging of standing (stagnant) water. This was done by using a low flow pump at a discharge rate of 0.20 L/s. Temperature and electrical conductivity (EC) were continuously measured and monitored in the purged water. Samples were only collected after stabilization of the temperature and EC, which generally occur after purging of the double of the volume of standing water in the monitoring borehole. At each sampling point, the sampler wore latex examination gloves, and prior to sample collection, bottles were rinsed with hydrochloric acid at a pH of 2.00 to remove leachable material. Water samples were collected in standard 1 L polyethylene bottles, and were tightly closed to protect from atmospheric gases. Thereafter the samples were labelled and stored in a cooler box (<4 °C).

In the four year monitoring period, one thousand nine hundred and twenty samples were collected monthly from a total of forty three monitoring boreholes drilled into a shallow weathered/fractured groundwater system in and surrounding the open pit mining area.

3.2. Chemical analysis

Chemical analysis was conducted by Cap Vet Laboratory, a local SANAS accredited laboratory in Mokopane (South Africa). The guidelines provided in the Standard Methods for the Examination of Water and Wastewater (American Water Works Association et al., 2005), were followed to conduct the samples analysis. Most of the analysis methods reflect SANAS accredited analysis methods. All samples were filtered using 0.45 μm Millipore membrane filters, and were then were analyzed for major and minor ions, as well as heavy metals. Calculated ionic balance error for the analyses ranged between±2% to ±17%. Samples with an ionic error balance greater than 5% and less than −5% were omitted in further analysis. The errors may be associated either to sampling procedure, laboratory analyses procedures, or reporting.

4. Data processing and computation

Piper (Walton, 1962; Piper, 1944) and Expanded Durov (Burdon and Malzoum, 1958) diagrams were used in order to categorize the samples into various Hydro-geochemical types and facies. These diagrams graphically demonstrate relationship between the most important dissolved constituents in a set of groundwater samples. For more details on how to read this diagrams can be found in Freeze and Cherry (1979). Scatter diagrams, multivariate plots (Abid et al., 2010), and Pearson Product Moment (PPM) correlation coefficients between chemical ion concentrations were plotted. The hydro-geochemical model PHREEQC was used to compute (calculate) the Saturation indices (SI) for the different mineral phases (Parkhurst and Appelo, 1999).

5. Results and discussion

Major ions concentration in the groundwater, were detected in the following order $HCO_3^- » Cl^- » Mg^{2+} » NO_3^- » F^-$. The descriptive statistics of the major ions detected in the Platreef's groundwater system during the monitoring period are summarized in Fig. 6.

The pH measured in the groundwater samples during the monitoring period range from 5.60 to 9.27 (Fig. 7). Due to the pH values being below 9.70 (Fig. 7), it is assumed that alkalinity is accredited to the dissolution of Carbonate (i.e., Alk = $[HCO_3^-\text{total}] + 2[CO_3^-\text{total}]$).

5.1. Hydro-geochemical types associated with the Platreef

04 different hydro-geochemical types are identified from the analyzed of Expanded Durov (ED) diagrams. The corresponding hydro-geochemical facies on the Piper diagram are also discussed.

The Expanded Durov diagrams show that the groundwater system in the region is mainly characterized by “non-dominants ions” hydro-geochemical type (Figs. 8 and 9). 45% of the analyzed samples fall under Field 5 of the ED diagram. This indicates that dissolution or mixing processes are mainly occurring in the groundwater system. The Piper diagram plot of these “non-dominants ions” samples, confirms that no specific cation-anion pair exceeds 50% of the total dissolved elements.

Freeze and Cherry (1979) suggest that when no dominant water type is present, then the possibility of mixing of two chemically distinct waters is possible. In this scenario this mixing could be attributed to freshly recharged water and contamination. Furthermore, 30% of these samples show water of static regimes with combined concentrations of Sulfate, Chloride, and magnesium exceeding 50% of their respective total mEq/L (Fig. 10).

Bicarbonate magnesium (HCO_3^- and Mg^{2+}) water type constitutes the second most dominant hydro-geochemical type in the groundwater system. 34% of the analyzed samples fall under Field2 of the ED (Fig. 9). This suggests water associated with dolomite (of Transvaal Super Group) or mafic igneous rocks of the Bushveld complex, depending on the location of the sampled boreholes. The combined concentration of calcium, magnesium and bicarbonate exceed 50% of their respective total mEq/L. Such samples show

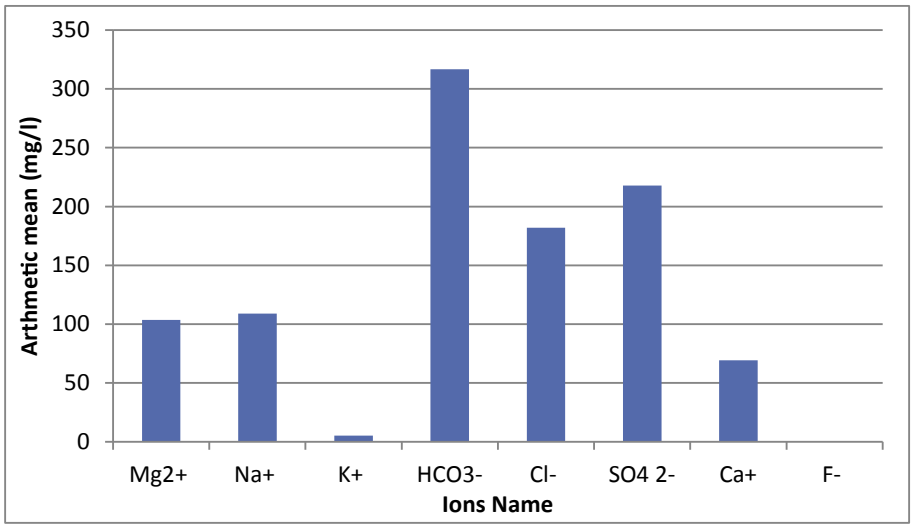

Fig. 6. Majors ions concentrations.

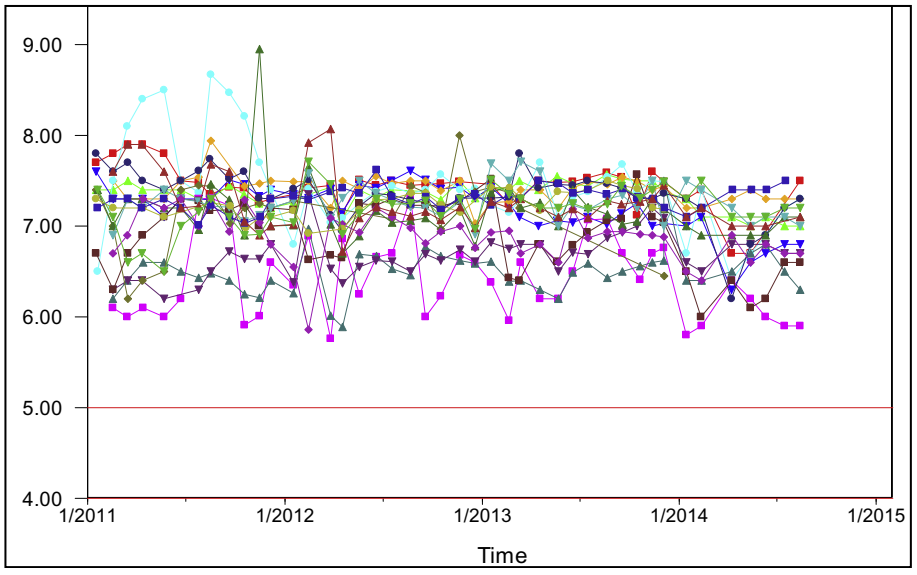

Fig. 7. pH measured in the samples collected from borehole with linear trends on Piper diagram.

(Fig. 11) some hardness (plotting left side of Piper diagram's diamond), and so suggest recently recharged water. Note that the magnesium may be the main source of the "hardness", since there is a tendency towards lower calcium concentrations. Dominant magnesium-bicarbonate waters in the study area may be explained by the abundance of ferromagnesian minerals within the rocks (Holland, 2011).

The sodium bicarbonate (HCO_3^- and Na^+) water type constitutes 14% of the analyzed samples. This corresponds to Field 3 on the ED, which suggests that ion exchange is the dominant process occurring in the groundwater system. Sodium Bicarbonate type water is one of the dominants on the Plateau (Holland, 2011). This is probably formed by cation exchange with sodium-rich clay minerals. Alternatively it could be due to the weathering of albite to kaolinite in the crystalline rocks, releasing sodium and bicarbonate.

Minor hydro-chemical types, which plot as sulfate-sodium (SO_4^{2-} and Na^+), chloride (Cl^-), chloride-sodium (Cl^- and Na^+), and chloride-calcium (Cl^- and Ca^{2+}) constitute less than 7% of the samples. These hydro-chemical groundwater types are probably a reflection of the mixing, and chemical evolution processes that occur as the groundwater evolves to the calcium sulfate ($Ca^{2+} - SO_4^{2-}$) hydro-chemical type.

More than 60% of the sampling points (boreholes) show linear correlation trends on the Piper Diagram Plots (Figs. 10–12). One can therefore use such linear dependence to infer the chemical reaction/processes which result in the main hydro-geochemical types. In addition to this, most of the boreholes showing these trends are located down gradient of waste rock dumps, tailing and dirty water dams.

5.2. Hydro-geochemical processes within the monitoring area

The focus here is on the hydro-geochemical reactions and processes that result from the dominant water quality types associated with the Platreef and the subsequent to mining activities.

Knowing that the majority (90%) of the boreholes from which

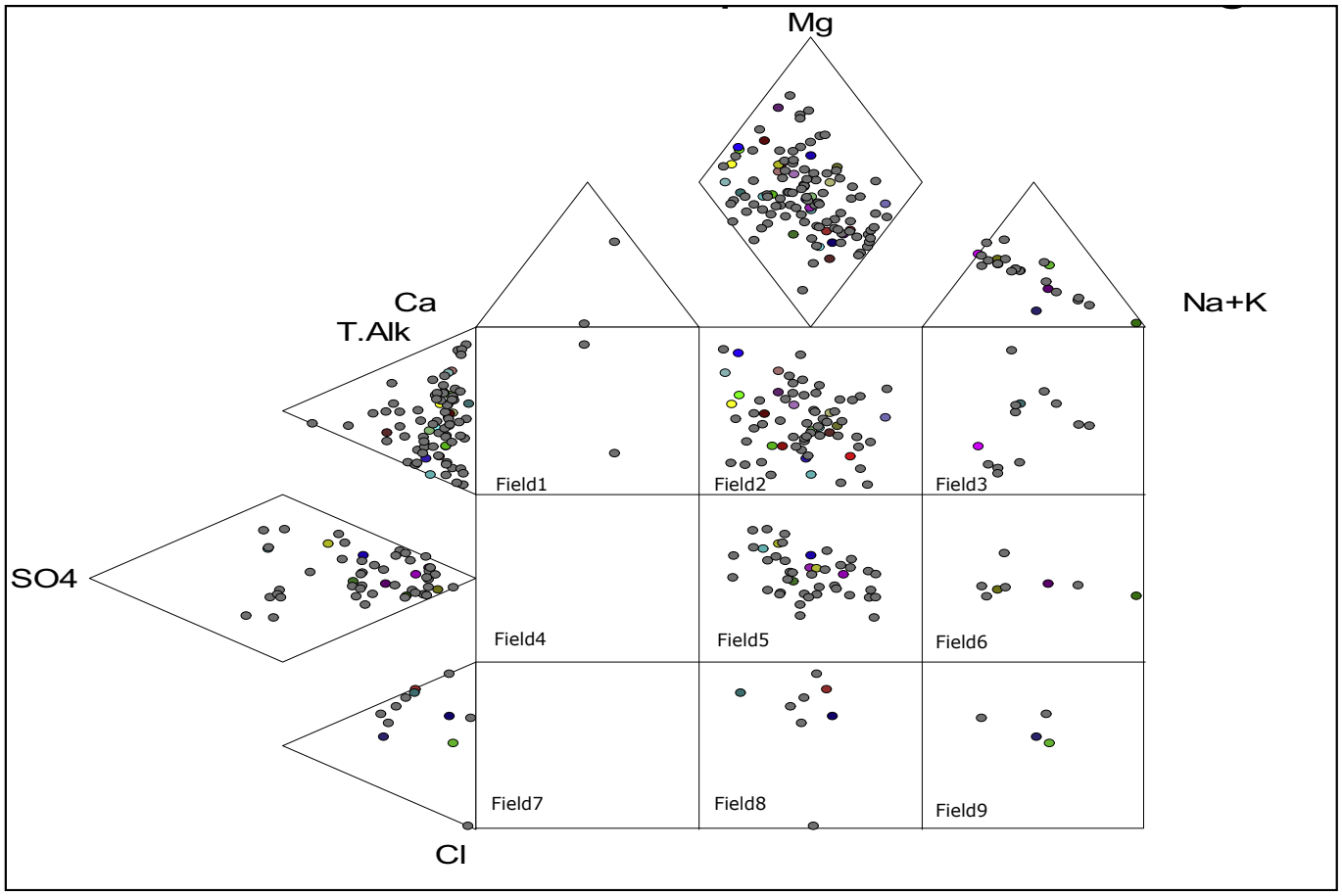

Fig. 8. Expanded Durov diagram of the samples in the entire catchment.

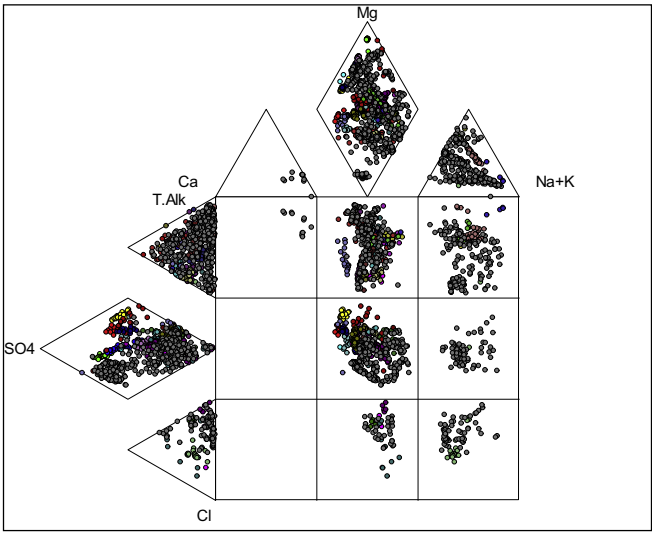

Fig. 9. Expanded Durov diagram of the samples in the monitoring area (04 years).

groundwater have been sampled, are less than 70.00 m deep; and considering the local topography and drainage, we assume the sampled aquifer system is directly recharge by the rainwater. This is confirmed by the Trilinear/Piper Diagram showing the maximum of the samples is from freshly recharge type. Furthermore rain water quality in the region is known to be mostly of Calcium Bicarbonate type (Holland, 2011), but how does rainwater (general) evolve to the different main hydro-geochemical types that occur in the catchment?

A same hydro-chemical groundwater type can result from various rock-mineral and water reaction processes. One needs to develop a sound hydro-geochemical conceptual model (Fig. 19) based on the site geology, hydrogeology, and mineralogy. One also needs to assess (test) the validity of each hypothetically conceived reaction based on measured chemical data. This is done for main hydro-geochemical types occurring in the catchment.

We are only interested in relating the observed dominant water type to the most probable rock-mineral and water reactions, through thermodynamic chemical reactions, since the chemical reactions are fast relative to the hydrological processes.

Significant groundwater levels fluctuations occurred during the monitoring period, probably in response to the recharge and discharge cycles that occur during the wet and dry seasons. During the monitoring period, overall constant rising trends of the groundwater levels are observed in boreholes located close to tailing dams. Fig. 13 illustrates such trends from selected boreholes. This constant rising suggests an artificial groundwater recharge, in form of water infiltration from the tailing dams.

Bicarbonate is the most abundant ion (anion) in the hydro-geochemistry of the Platreef. The sources of carbonate minerals are ubiquitous in our environment. Rainwater is a source for bi-carbonate ions, but is probably not a major chemical contributor to the system Silicate weathering products may constitute the major source of Bicarbonate, Furthermore, CO_2 dissolved in rain water

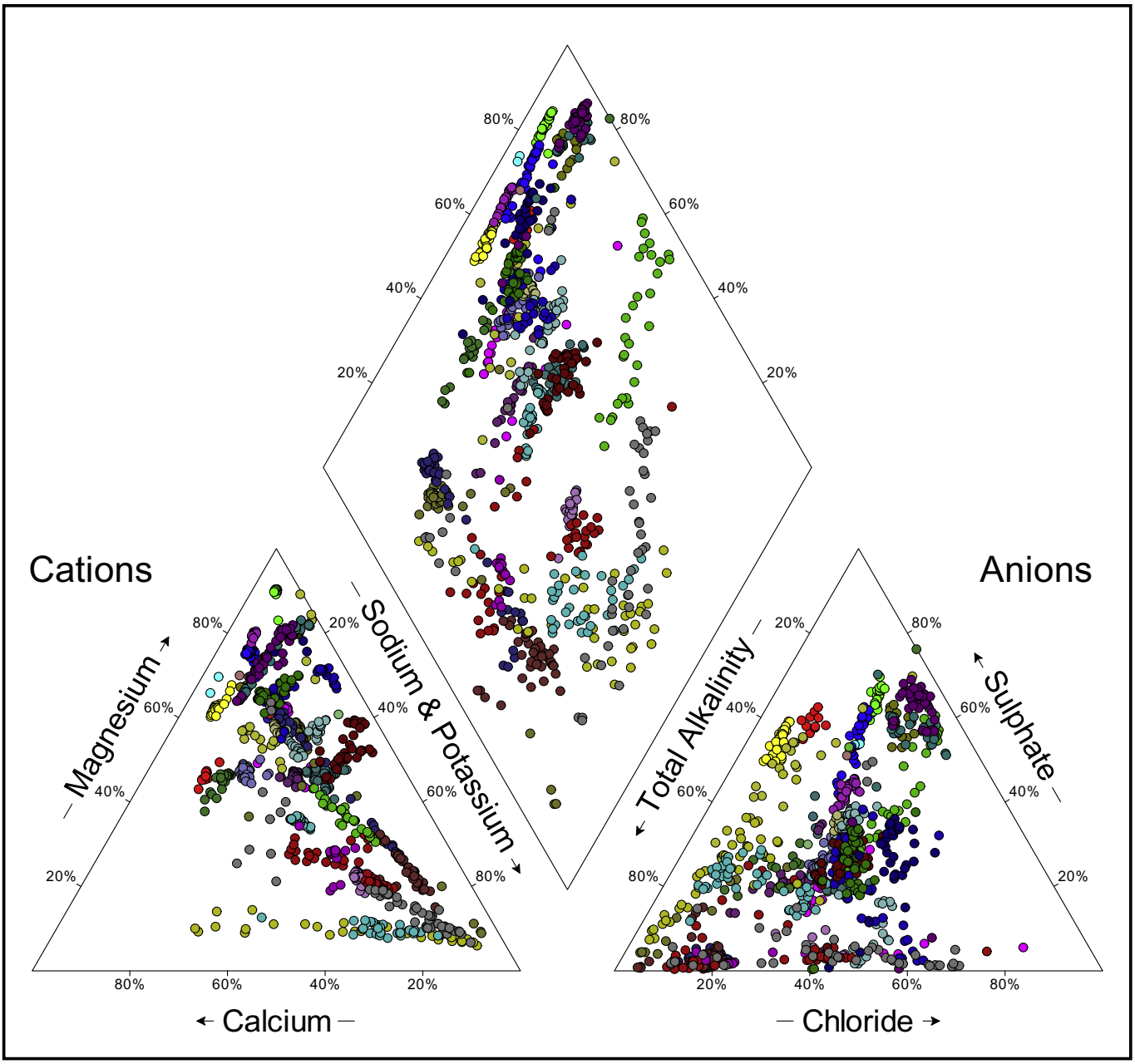

Fig. 10. Piper diagram of samples representative of Non dominant type.

may form carbonic acid, which in turn may dissociate to form bicarbonate and hydrogen ions, depending on the buffering capacity of the groundwater. One also has to bear in mind that, the alkalinity and acidity of groundwater might be influenced by other constituents (organic acids, phosphates, etc.). Bicarbonate (HCO_3^-) is a function of pH and salinity. It's content in the groundwater changes as function of pH.

5.2.1. Acid mine drainage in the Platreef

The previous work completed in the area alludes to the PGE in the area having a low AMD potential (Foose et al., 1995). This is due to their trend of low sulfide abundances. The Platreef is characterized by extensive amounts of base metal sulfides, which occur in the following decreasing order of abundance pyrrhotite, pentlandite, chalcopyrite and minor pyrite (Foose et al., 1995; Kinnaird and McDonald, 2005).

Acid Base Accounting investigation, demonstrates that some of the rocks to be mined and the tailings material to be generated (from beneficiation) at the Platreef, includes low risk as well as high risk acid generating material (Lishman, 2009). Some rocks samples and tailings samples contain more than 0.30% sulfide-sulfur and are classified as high risk acid producing potential (Lishman, 2009). These rocks samples include Pegmatitic Gabbro-Norite, Melanorite, Norite Cycles and Feldspathic Pyroxenite. Soregaroli and Lawrence (1998) demonstrated that rock material with at least 0.30% sulfide-sulfur content may generate acid, if exposed to the atmosphere (oxidation) for extended periods of time. Open and exposed (to atmosphere) fractures in the Marginal Zone Norite and Hornfels of the footwall of the Platreef, and the associated xenoliths in the Platreef, are likely to allow the oxidation of the base metal sulfides,

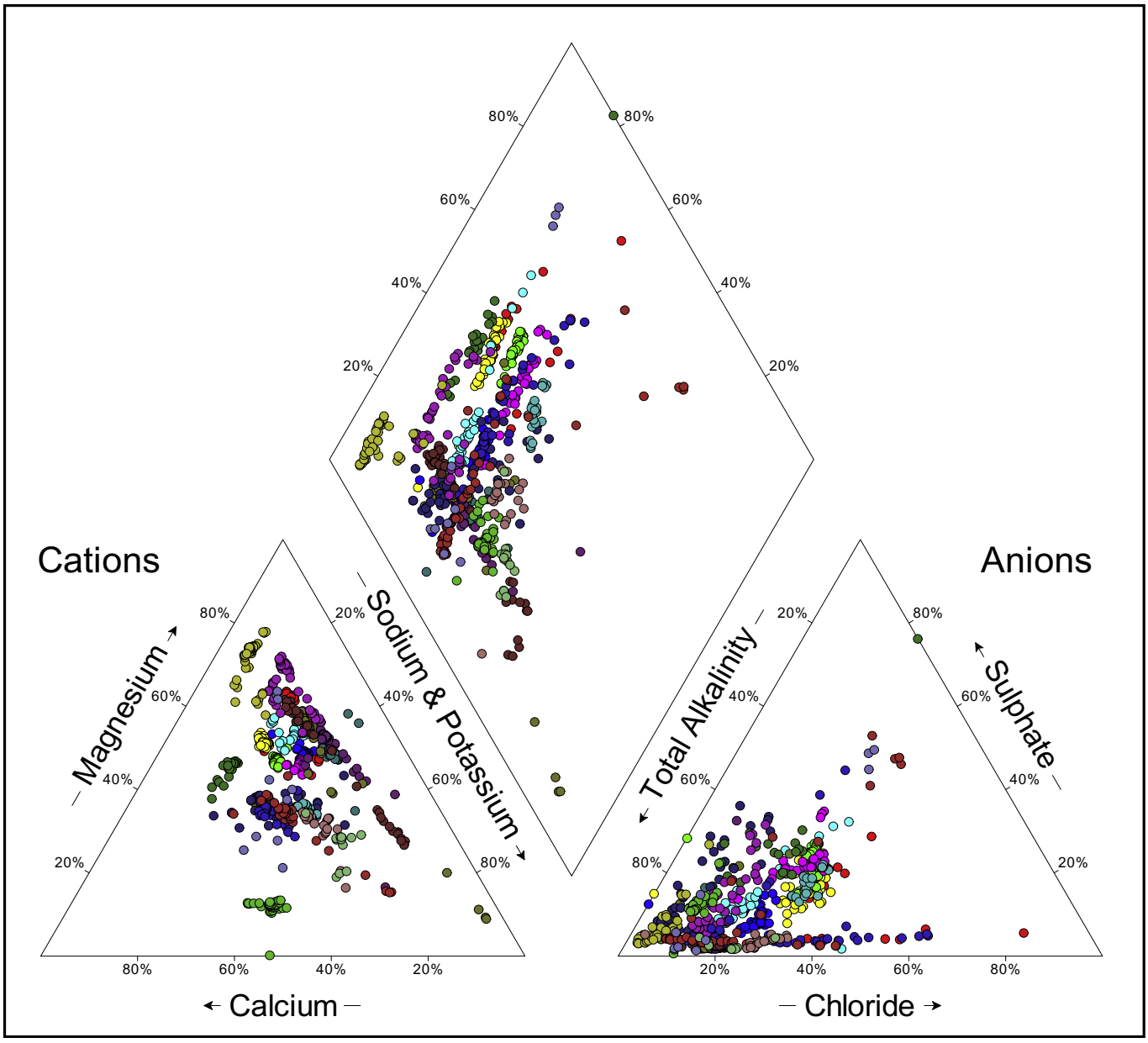

Fig. 11. Piper diagram of samples representative of Bicarbonate Calcium magnesium type.

provided it is exposed for longtime.

5.2.2. Pyrrhotite oxidation

Sulfate (SO_4^{2-}) appeared to constitute the second most abundant ion (anion) in the investigated area. The overall series of reactions that lead to acid production from pyrrhotite oxidation is described by the reaction presented from equation (1) to equation (3) (Benner et al., 2000; Blowes et al., 2003 Belzile et al., 2004). At pH > 4.00, Oxygen is the ultimate oxidant (direct) of sulfide minerals in presence of water, but at low pH (<4.00) sulfides are oxidized by ferric iron (Nordstroom and Alpers, 1999). Due its relatively poor ordered structure, pyrrhotite shows variations in chemical stoichiometry, and nonstoichiometric and stoichiometric compositions exist in which x in the formula $Fe_{(1-x)}S$ can vary from 0.125 (Fe_7S_8) to 0 (FeS).

$$Fe_{1-x}S + \left(2 - \frac{x}{2}\right)O_2 + xH_2O \rightarrow (1-x)Fe^{2+} + SO_4^{2-} + 2xH^+ \quad (1)$$

The ferrous iron is then oxidized to form ferric ions that can precipitate out solution to form ferric hydroxide at pH > 4.00.

$$Fe^{2+} + \frac{1}{4}O_2 + 2H^+ \rightarrow Fe^{3+} + \frac{1}{2}H_2O \quad (2)$$

The ferric ions are then oxidized by oxygen and precipitated as ferric hydroxides.

$$Fe^{3+} + 3H_2O \rightarrow Fe(OH)_{3(s)} + 3H^+ \quad (3)$$

Atmospheric oxidation of pyrrhotite results in acid, sulfate and iron, the latter potentially as a solid. Trace metals may be dissolved

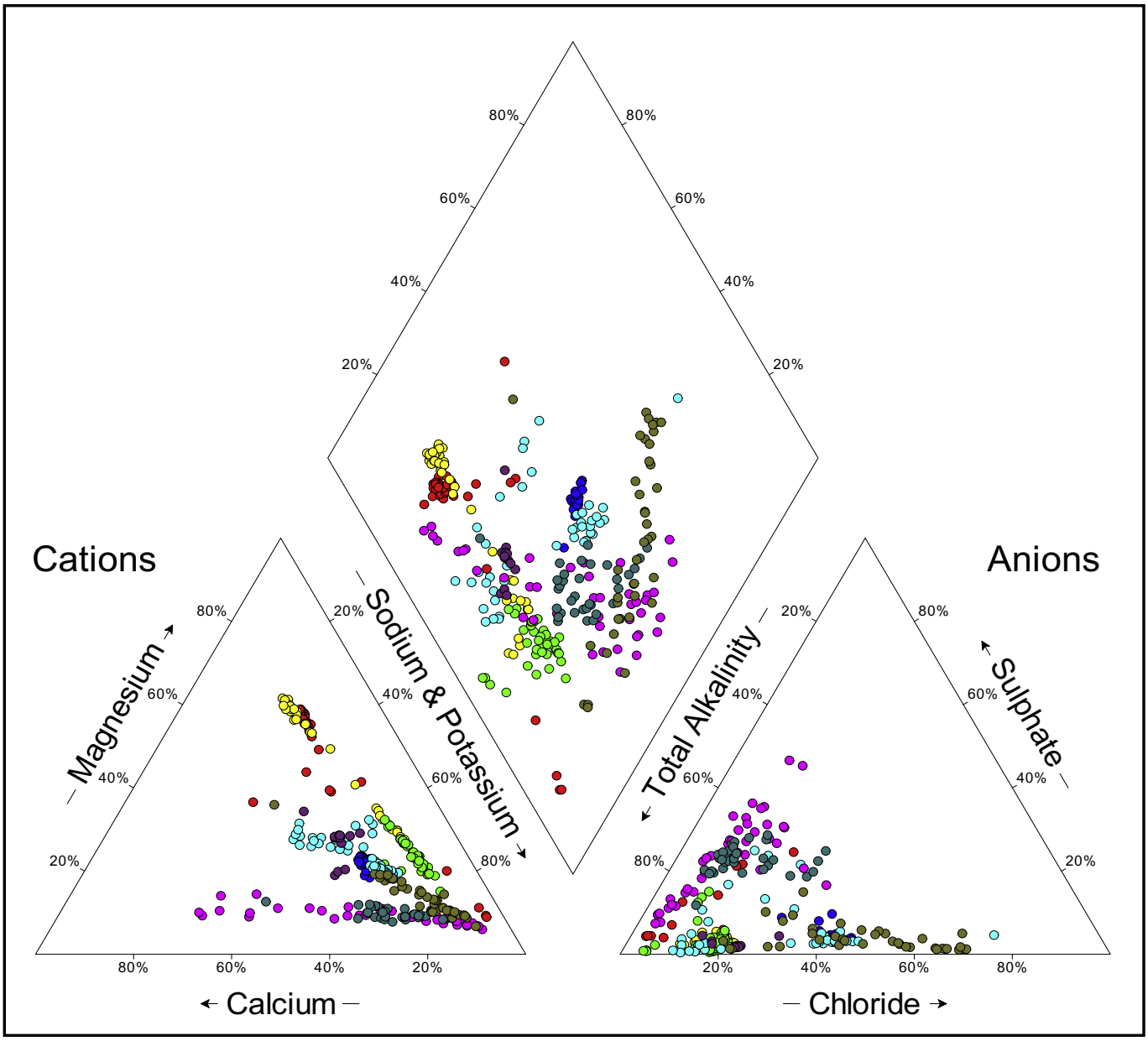

Fig. 12. Piper diagram of samples representative of Bicarbonate Sodium type.

by acid from other minerals. Considering then ferrous irons and ferric ions oxidized simultaneously with reaction of Equation (1) and then Equations (2) and (3) can be thermodynamically combined with Equation (1) and be represented with reaction shown in Equation (5), for $x = \frac{1}{8}$

$$Fe_{\frac{7}{8}}S + \frac{35}{8}O_2 + \frac{21}{8}H_2O + \frac{1}{8}Fe^{2+} \leftrightarrow SO_4^{2-} + \frac{45}{20}H^+ + Fe(OH)_{3(s)} \quad (4)$$

5.2.3. AMD buffering

AMD processes generally occur by co-existing buffering mechanisms that can prevent drops in the pH. More than 90% of the groundwater samples showed pH values that fluctuated between 6.00 and 8.50 (Fig. 9) over the monitoring period. Under such measured pH ranges, serpentinite, calcite and dolomite minerals can be dissolve, and buffer AMD. The Gabbro-Norite and Mottled Anorthosite of the Platreef's Hanging-wall, the dolomite of the Footwall, and serpentinite associated with the PGE, have a neutralizing (Buffering) capacity. This was established by Lishman (2009).

5.2.3.1. Serpentinite buffering. Rocks in the study area are serpentinized at various degrees, and contain graphite-bearing serpentinite (Bye and Bell, 2001; Armitage et al., 2002; McDonald et al., 2005). Serpentine constitute also one of the main filling minerals of various continuous joints observed in the Plaatreef. These joints constitutes preferential flow path for water after heavy rainfall (Bye and Bell, 2001). In acidic water (pH < 7.00), cations from the silicate minerals (serpentinite) dissolve, and its dissolution Equation (5) is followed by nucleation and precipitation of carbonate (Guthrie et al., 2001; Chizmeshya et al., 2003; Teir et al., 2007; Jarvis et al.,

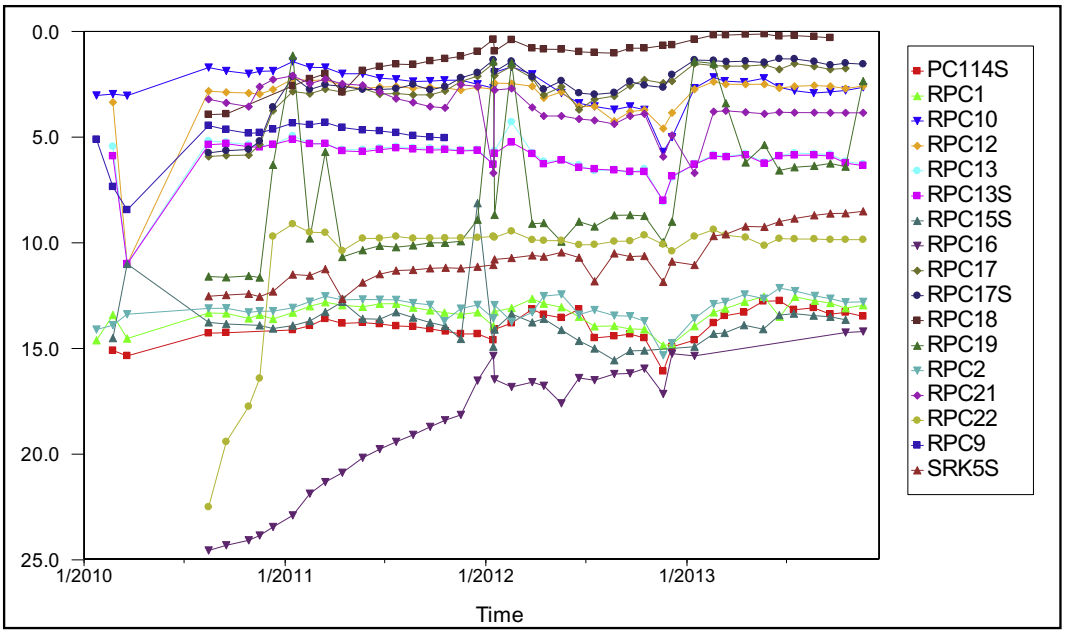

Fig. 13. Evolution of depth to groundwater levels.

2009).

$$Mg_3Si_2O_5(OH)_4 + 6H^+ \leftrightarrow 3Mg^{2+} + 2SiO_{2(aq)} + 5H_2O \quad (5)$$

$$Mg^{2+} + HCO_3^- \rightarrow MgCO_{3(S)} + H^+ \quad (6)$$

5.2.3.2. Calcite and dolomite buffering. We investigate base on multivariate plots, the plausibility of Calcite and Dolomite dissolutions investigations as part of dominant acid buffering reactions in the groundwater system. The plot of $SO_4^{2-} + HCO_3^-$ versus $Mg^{2+} + Ca^{2+}$, will have a slope close to the 1:1, provided the dissolutions of calcite and dolomite by sulfuric acid are the dominant reactions in a system (Guler et al., 2002; Gomo et al., 2012). Fig. 14 shows a scatter plot of $SO_4^{2-} + HCO_3^-$ versus $Mg^{2+} + Ca^{2+}$ concentrations observed in the groundwater system during monitoring period. The plot with slope 1.01 is very close to the 1:1 equiline. This confirms the dominance of dolomite and calcite dissolution as acid buffering reactions in the system, at the point of observations.

Calcite and dolomite buffering processes are dominant in the pH range of 6.50–7.50 (Blowes et al., 1994; Geller et al., 2000).

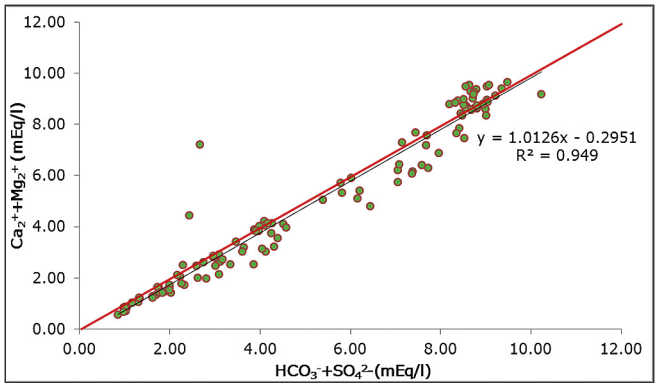

Fig. 14. Scatter plot showing (HCO_3^-+SO_4^{2-}) against (Ca^{2+}+Mg^{2+}) concentrations.

$$CaMg(CO_3)_2 + 2H^+ \leftrightarrow Ca^{2+} + Mg^{2+} + 2HCO_3^- \quad (7)$$

$$CaCO_3 + H^+ \leftrightarrow Ca^{2+} + HCO_3^- \quad (8)$$

Considering the co-existing (simultaneous reactions) buffering mechanisms and AMD processes, as described above; Equations (5), (7) and (8) can be thermodynamically combined with Equation (4) and be represented with reactions shown in the following respective equations:

$$Fe_{\frac{7}{8}}S + \frac{35}{16}O_2 + \frac{1}{8}Fe^{2+}Mg_3Si_2O_5(OH)_4 + \frac{15}{4}H^+ \leftrightarrow SO_4^{2-} + Fe(OH)_{3(s)} + 3Mg^{2+} + 2SiO_{2(aq)} + \frac{19}{8}H_2O \quad (9)$$

$$Fe_{\frac{7}{8}}S + \frac{35}{16}O_2 + \frac{21}{8}H_2O + \frac{1}{8}Fe^{2+} + CaMg(CO_3)_2 \leftrightarrow SO_4^{2-} + \frac{1}{4}H^+ + Fe(OH)_{3(s)} + Ca^{2+} + Mg^{2+} + 2HCO_3^- \quad (10)$$

$$Fe_{\frac{7}{8}}S + \frac{35}{16}O_2 + \frac{21}{8}H_2O + \frac{1}{8}Fe^{2+} + CaCO_3 \leftrightarrow SO_4^{2-} + \frac{5}{4}H^+ + Fe(OH)_{3(s)} + Ca^{2+} + HCO_3^- \quad (11)$$

Note that the molar ratios between the investigated Major chemical elements of the Bicarbonate-magnesium-calcium ($HCO_3^-Mg^{2+}$, and Ca^{2+}) will be produced from the chemical reactions of Equations (9)–(11) which are independent of order of the structure of the sulfate bearing mineral (pyrrhotite). So, for any value of x (between 0.13 and 0) in the formula $Fe_{(1-x)}S$, these molar ratios should be expected.

Equation (9) shows that when 1 mol of pyrrhotite is oxidized and co-exist with weathering and dissolution of serpentinite minerals, 1 mol of SO_4^{2-} and 3 mol of Mg^{2+} will be released into the solution. The reaction in Equation (10) shows that for every 1 mol of pyrrhotite oxidation, co-existence of dissolution of dolomite will

release 1 mol of SO_4^{2-}, 1 mol of Ca^{2+}, 1 mol of Mg^{2+}, and 2 mol HCO_3^- into the solution. Equation (11) shows that the calcite buffering of the acid produced by 1 mol of pyrrhotite oxidation will release 1 mol of SO_4^{2-}, 1 mol of Mg^{2+}, and 1 mol of HCO_3^- into the solution.

The reactions in Equations (9)–(11) may occur simultaneously, resulting in the production of 3 mol of SO_4^{2-}, 3 mol of HCO_3^-, 4 mol of Mg^{2+} and 2 mol of Ca^{2+} in the system. Alternatively, the reactions may occur in pair as follow:

- Equations (9) and (10) suggest: When 2 mol of SO_4^{2-} are produced, 2 Moles of HCO_3^-, 4 mol of Mg^{2+} and 1 mol of Ca^{2+} are produced in the system; (RPC12; RPC11; PC121S; PC122S);
- Equations (10) and (11) suggest: When 2 mol of SO_4^{2-} are produced, 3 mol of HCO_3^- , 1 mol of Mg^{2+} and 2 mol of Ca^{2+} are produced in the system;
- Equations (9) and (11) suggest: When 2 mol of SO_4^{2-} are produced, 1 mol ofHCO_3^-, 3 Moles of Mg^{2+} and 1 mol of Ca^{2+} are produced in the system.

Fig. 15 shows a scatter plot of observed HCO_3^- against Ca^{2+} and Mg^{2+} PPM during monitoring period. HCO_3^- is positively correlated to Ca^{2+} and Mg^{2+} with correlation coefficients of 0.95 and 0.96 respectively, confirming that these three ions have the same linear time evolution in the groundwater system.

In a groundwater system controlled by the reactions of Equations (9)–(11) the molar ratio of Ca^{2+} and Mg^{2+} to HCO_3^- should be 1:2; and the molar ratio of Mg^{2+} to Ca^{2+} should be 1:1. Plots of Ca^{2+} against HCO_3^-, Mg^{2+} againstHCO_3^-, and Ca^{2+} against Mg^{2+} would have slopes of 0.50, 0.50, and 1.00 respectively. These predictions are close to slopes (0.51, 0.50, and 0.99 respectively) of such plots for observed values which (Figs. 15 and 16). This indicates that there is no distinct dominant buffering reaction.

5.2.4. Ions exchanges of sodium for calcium and magnesium

The plot of the observed concentrations of $SO_4^{2-} + HCO_3^-$ versus $Mg^{2+} + Ca^{2+}$ (Fig. 14) shows a shift to the right side of the 1:1 line ($SO_4^{2-} + HCO_3^-$), which is an indication of ion exchange processes taking place in the system (Fisher and Mulican, 1997). The shift in the plot could be attributed to the decreasing amounts of Mg^{2+} and Ca^{2+} in the groundwater as they occupy exchange sites occupied by Na^+. In addition, it is expected that if meteoric $NaCl$ is the source of Na^+ in the groundwater system, then a plot of Na^+ against Cl^- in the groundwater should fall on the 1:1 evaporation line (Gomo et al., 2012). The plot of Na^+ against Cl^- (Fig. 17) shows that groundwater samples at the site are located above (on left of) the 1:1 evaporation line. This implies that rainfall is not the only source of Na^+ in the groundwater water system, which means that Na^+ concentration is increased by other occurring process. Jankowski and Beck (2000) reported that a shift of fro the previously mentioned evaporation line could be attributed to the addition of Na^+ ion in to the groundwater by means of ion exchange.

Jankowski and Beck (2000) explained that in a system dominated by ion exchange processes, the plots of (Mg^{2+}+Ca^{2+}-SO_4^{2-}-HCO_3^-) versus ($Cl^- - Na^+$) should form a line

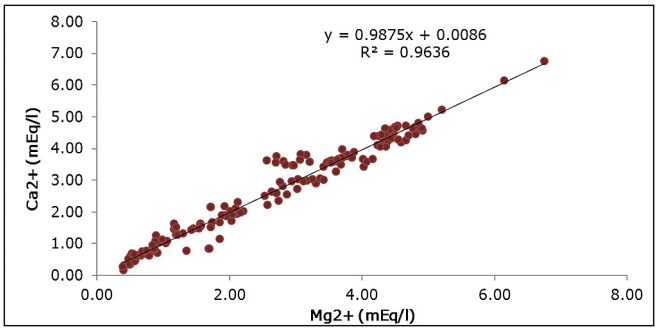

Fig. 16. Scatter plot showing Ca^{2+} against Mg^{2+} concentrations.

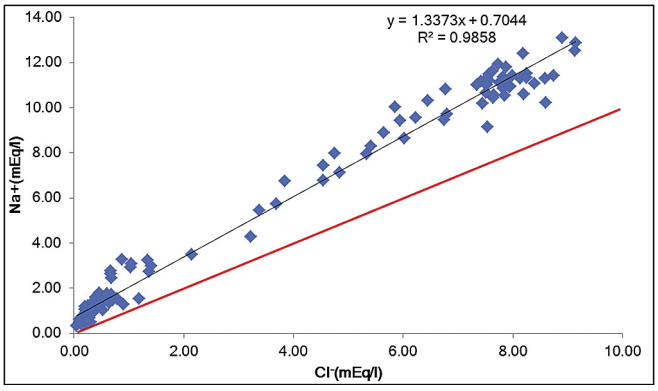

Fig. 17. Scatter plot showing Cl^- against Na^+ concentrations measured during monitoring period.

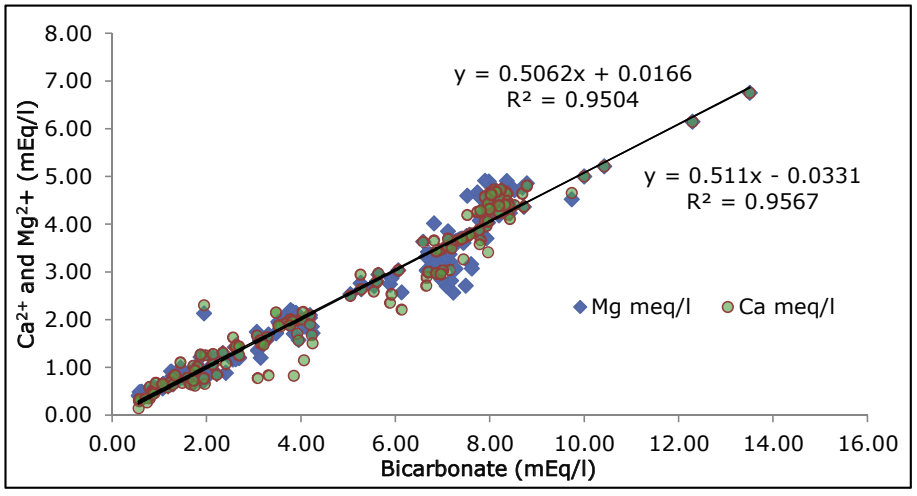

Fig. 15. Scatter plot showing HCO_3^- against (Ca^{2+} and Mg^{2+}) concentrations.

with slope of −1. According to Jankowski and Beck (2000), by subtracting chloride from sodium chloride (considering that Cl^- is a conservative ion, and assuming that all Cl^- comes from precipitation), groundwater that is not influenced by the ion exchange will plot close to zero on this axis. When ($SO_4^{2-} + HCO_3^{2-}$) concentration are subtracted from ($Mg^{2+} + Ca^{2+}$) concentrations, the dissolution of calcite, dolomite should also return values of zero assuming that dissolution occurs at the same rate and no ion exchange occurs.

The plot of Mg^{2+}+Ca^{2+}-SO_4^{2-}-HCO_3^- versus $Cl^- - Na^+$ has an observed slope of −1.04 as well as correlation coefficient of 0.93, thus highlighting the evidence for ion exchange processes occurring the aquifer (put a reference in or make reference to similar studies (Fig. 18)).

The cross section of the hypothetical hydro-geochemical model in the area is illustrated in Fig. 19.

5.3. Saturation state

The saturation Index (SI) is a useful measure of saturation of the water with respect to a given mineral (Deutsch, 1997). When the mineral solubility is in equilibrium (saturated) with the solution composition, the SI of the given mineral is equal to 0. Negative SI indicates that the mineral phase can dissolve and is undersaturated, while positive values reflect supersaturated hydrogeochemical conditions. The control of calcite, dolomite, and serpentine on geochemistry of Platreef's groundwater system within the monitoring area, were illustrated above. The inspection of the saturation indices of gypsum in relation to calcium, and sulfate can also help to better understand the trends of the measured concentrations of these ions in some samples of the system.

Using thermodynamic data contained in the database of the hydro-geochemical model PHREEQC (Parkhurst and Appelo, 1999), we calculated the SI for these minerals.

As it can be expected, linear (98%) relationship is observed between SIs (Fig. 20). This is explained by the direct dependence of SIs on the concentrations of the ions Mg^{2+},Ca^{2+} andHCO_3^-. This correlation confirms that the reactions of the two minerals are controlled by similar hydro-geochemical process (Gomo and Vermeulen, 2014).

In the majority (more than 60%) of the samples, calcite and dolomite are under saturated and tend to dissolve in the groundwater system (Fig. 21). These dissolutions occur at pH < 7. There is also a constant increase of the SI of the carbonate minerals with pH (Fig. 21). The alkalinity produced during the neutralization of AMD results in the increase in pH.

The plots of dolomite SI and Calcite SI in function of the evolution of measured concentrations of Mg^{2+} and Ca^{2+} are presented in Figs. 22 and 23 respectively. These plots suggest that Mg^{2+} and Ca^{2+} in the mine's groundwater system would only occur up to certain points. At these points their respective aqueous solubility will become limited by the saturation of calcite and dolomite. The mine's groundwater becomes saturated with respect to calcite at the concentrations above 2.50 mEq/L and 3.00 mEq/L for Mg^{2+} and Ca^{2+} respectively (Fig. 22). The mine's groundwater becomes saturated with respect to dolomite at the concentrations above 2.00 mEq/L and 3.00 mEq/L for Mg^{2+} and Ca^{2+} respectively (Fig. 23). Saturations lead to precipitations of dolomite and calcite and tend to reduce magnesium and calcium in the system.

Analytical results of the water extracts of some composites samples obtained from tailings dam in the area suggested that the sulfate may be present predominantly as gypsum, considering the relatively low levels of Na (Schwegler, 2003). The inspection of gypsum SI shows that the groundwater in the monitoring area and during the monitoring period, remains under saturated with respect to gypsum. This implies gypsum dissolution, and suggests gypsum may be contributing to the calcium and magnesium of the system. However the plot of gypsum SI against measured concentrations of calcium and sulfate do not support such a hypothesis (Fig. 24). The lack of linear relationship between calcium and sulfate concentrations in the system also rejects the hypothesis that calcium and sulfate concentrations in the system may be linked to gypsum (Fig. 25).

Fig. 24 shows that a similar trend exists between the respective changes of the concentrations of calcium against gypsum SI. This is simply because magnesium concentrations in the groundwater were changing in a similar trend with calcium as controlled by the carbonate minerals AMD buffering. It is another evidence to prove that carbonate AMD neutralization reactions are the main source of calcium, magnesium and sulfate, and not gypsum dissolution. Groundwater quality.

The oxidation of sulfide minerals during acid mine drainage releases acid sulfate and metals into the groundwater system and these can affect the resultant groundwater quality. Carbonate acid neutralization processes can also release elevated cations into the groundwater system and these can also contribute to the evolving

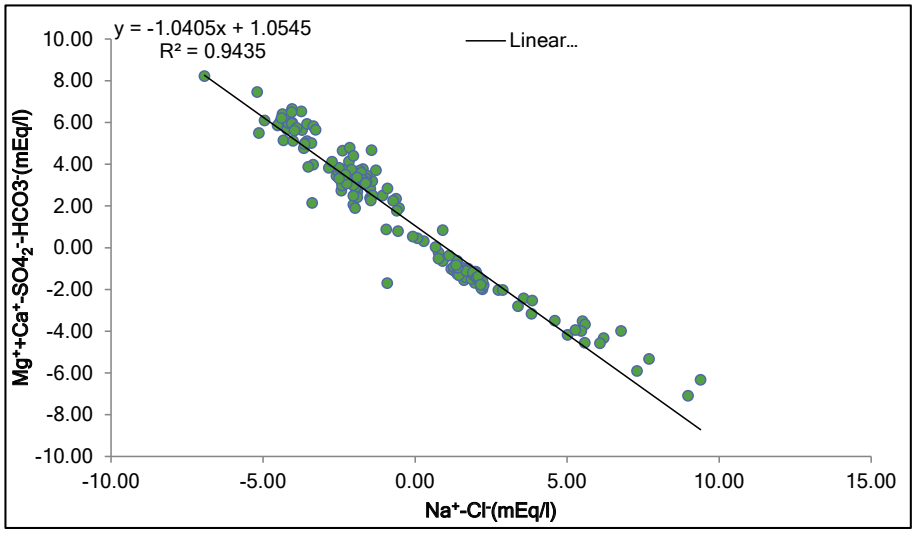

Fig. 18. Scatter plot showing (Mg^{2+}+Ca^{2+}-SO_4^{2-}-HCO_3^-) against ($Cl^- - Na^+$).

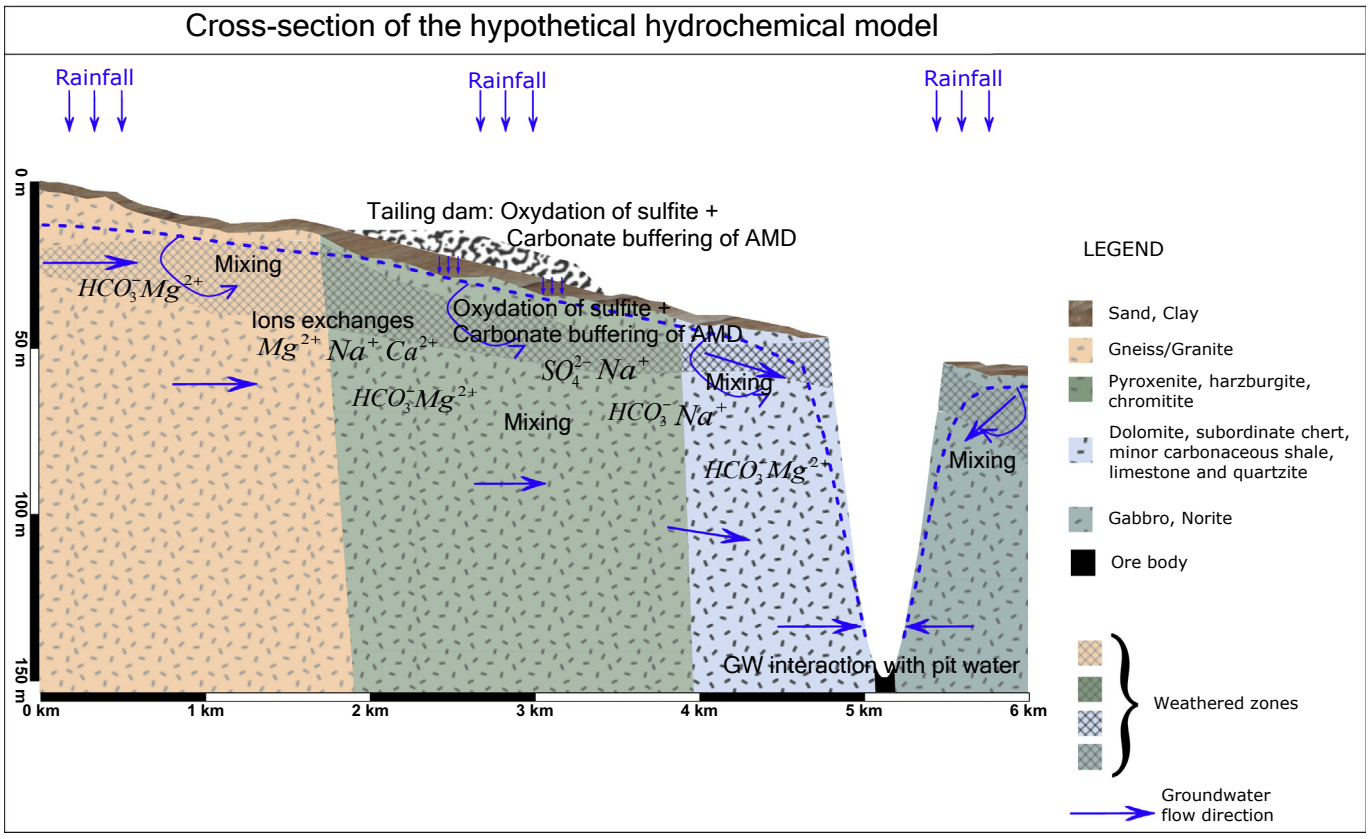

Fig. 19. Cross section of the hypothetical hydro-geochemical model in the area.

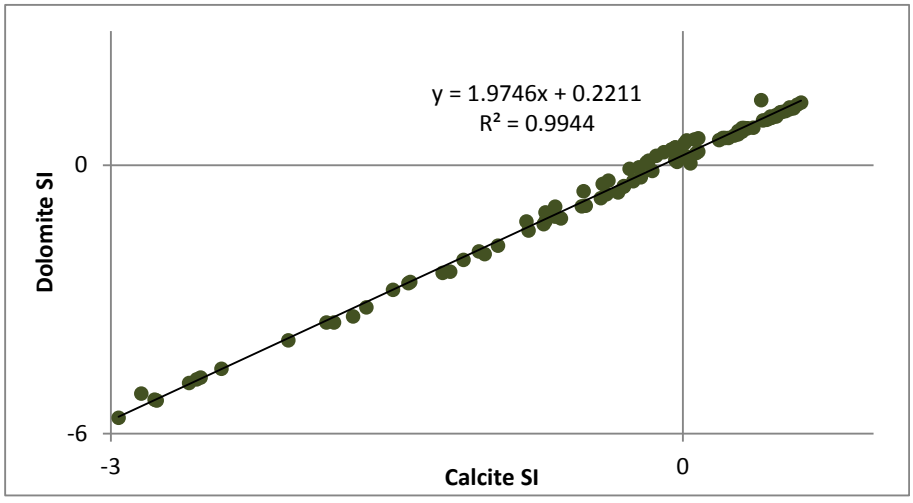

Fig. 20. Scatter plot of Dolomite SI against Calcite SI.

groundwater quality.

5.3.1. Metals

We have demonstrated above how the observed groundwater quality may have evolved from the oxidation of pyrrhotite and subsequent buffering reactions. Pyrrhotite is the next most abundant iron sulfide (Following pyrite) in nature (Lishman, 2009; Belzile et al., 2004). Acidic water which is generated from oxidation of pyrrhotite may content high concentrations of dissolved metals (Johnson et al., 2000; Ekosse et al., 2004). Elevated concentrations of metals pose a potential risk of groundwater quality deterioration (Blowes et al., 1994; Rose and Cravotta, 1998). The levels of metal concentrations in a groundwater system that might have hydro-geochemically evolved through AMD were therefore assessed. Considering the geology in the area and the potential content of the waste materials (Fig. 19) focus were given to selected metals (Fe, Mn, Cu, Cd, Cr) that may dissolved into the water under acidic conditions, during monitoring period.

The arithmetic mean of the concentrations of metals that were detected in the Platreef's groundwater system during the

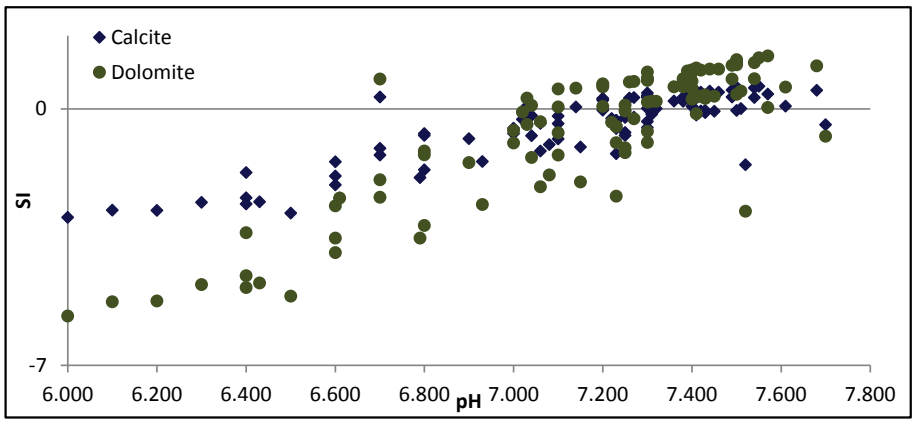

Fig. 21. Scatter plot of pH against dolomite and calcite SI.

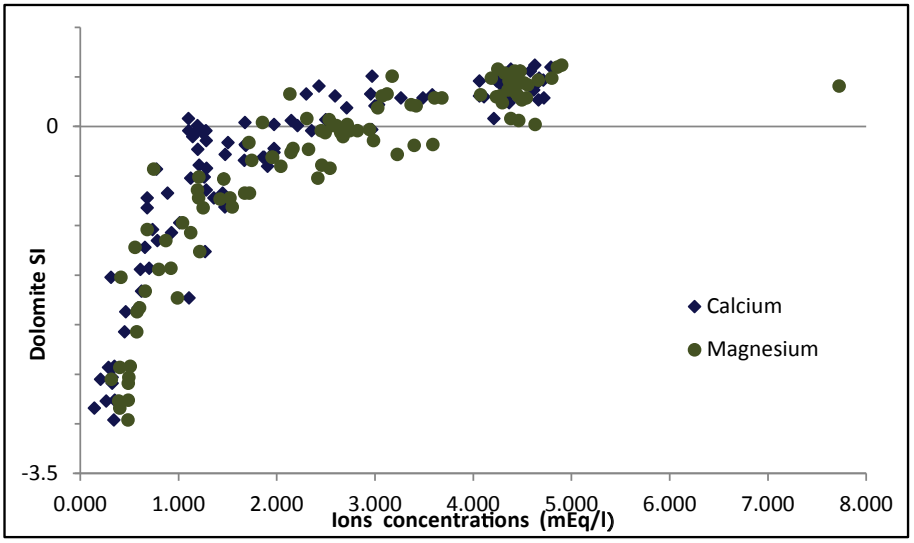

Fig. 22. Scatter plot of dolomite SI against Mg^{2+} and Ca^{2+}.

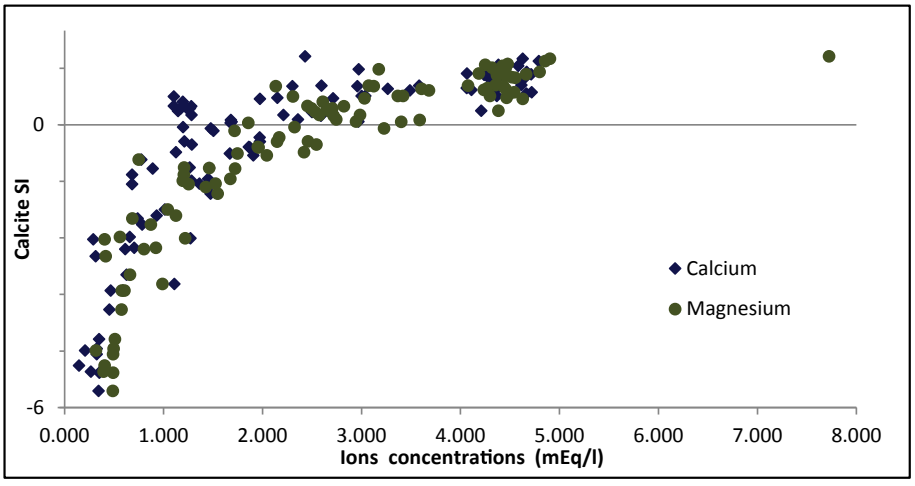

Fig. 23. Scatter plot of calcite SI against Mg^{2+} and Ca^{2+}.

monitoring period are summarized in Fig. 26.

Measured metals concentration were compared to SANS-241 (2015) and WHO (2011) drinking water quality guidelines. It appears that *Fe* and *Mn* that exceeded the SANS-241 (2015) drinking water quality target concentration in 3% and 12% of the samples respectively. With such low percentage of samples of concerns, one

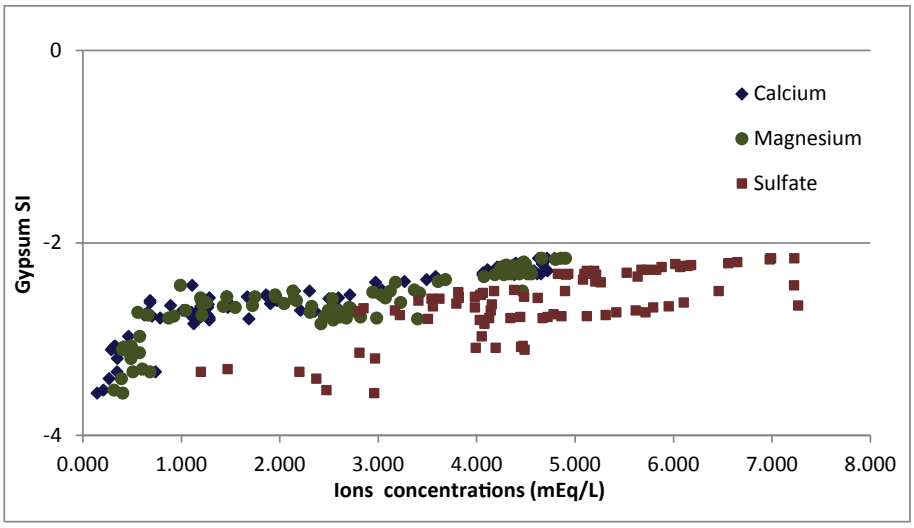

Fig. 24. Scatter plot of gypsum SI against Ca^{2+},Mg^{2+} and SO_4^{2-}.

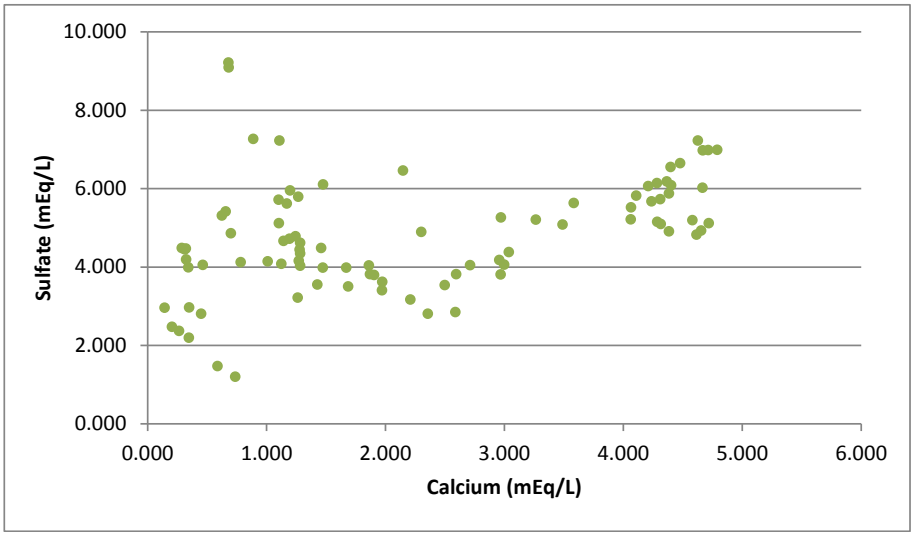

Fig. 25. Scatter plot of Ca^{2+} against Mg^{2+}.

cannot directly infer the presence of such forte concentrations of these dissolved metals (*Fe* and *Mn*) in some of the groundwater samples to the effect of AMD metal leaching. Especially not when, any hydro-geochemical background (Pre-mining) data could be found as reference. Except for these very few samples with elevated *Fe* and*Mn*, the rest of the assessed metals are generally all below the SANS-241 (2015) and WHO (2011) drinking water quality guidelines. It can therefore be concluded that the calcite and dolomite minerals in the PGE and base metals deposits are buffering the AMD thus preventing the leaching of metals into the sampled groundwater system.

5.3.2. Total dissolved solids (TDS) and total hardness

Fig. 27 shows the groundwater quality classification for the platinum mine area based on TDS levels (WHO, 2003). 73% of the groundwater samples have TDS in the acceptable range for drinking purposes (SANS-241, 2015). Only 54% of the samples are Excellent and/or Fair groundwater quality. The samples (27%) that fall under Poor to High classes of groundwater quality (greater than 900.00 mg/L) show also elevated concentration of $SO_4^{2-}Mg^{2+}$, and Ca^{2+} ions which were found to be released during the carbonate AMD buffering process.

Fig. 28 shows the classification of the groundwater quality in sampled area using calculated total Hardness the index developed by McGowan (2000). The majority (80%) of the groundwater samples have elevated hardness (total hardness > 180.00 mg/L). This is mainly due to the released of Mg^{2+} and Ca^{2+} ions into the system as result of AMD buffering process. Very hard water poses mainly the problem of aesthetic acceptability consumers and requires also economic and operational aspects to be considered (WHO, 2011).

The buffering minerals (Serpentinite, calcite and dolomite) are important for reducing the AMD levels and minimizing the potential leaching of metals into the mine groundwater system. The AMD neutralization also introduced a salinity problem in the aquifer, which represents vulnerability potentially for human use.

6. Conclusion

The study assessed, and described the foremost hydro-geochemical processes occurring at the open cast platinum mine.

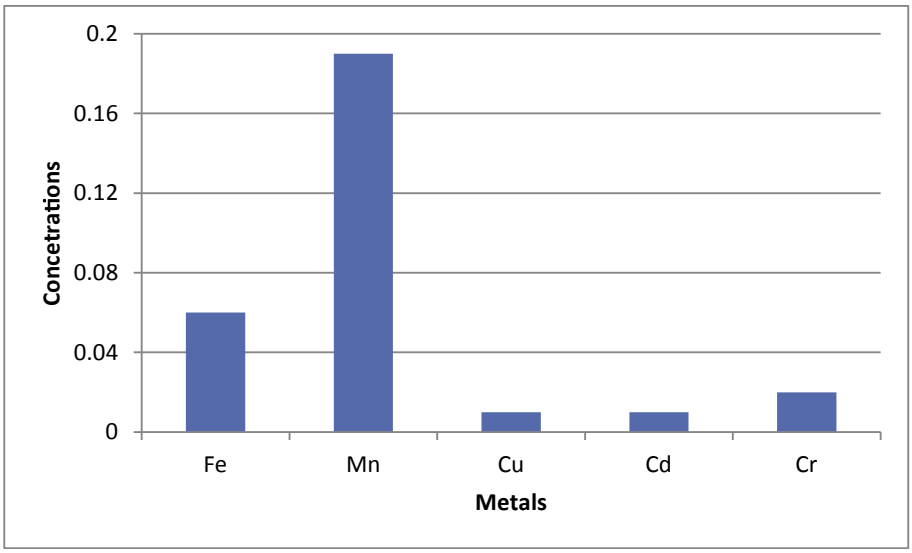

Fig. 26. Arithmetic mean of concentrations of metals.

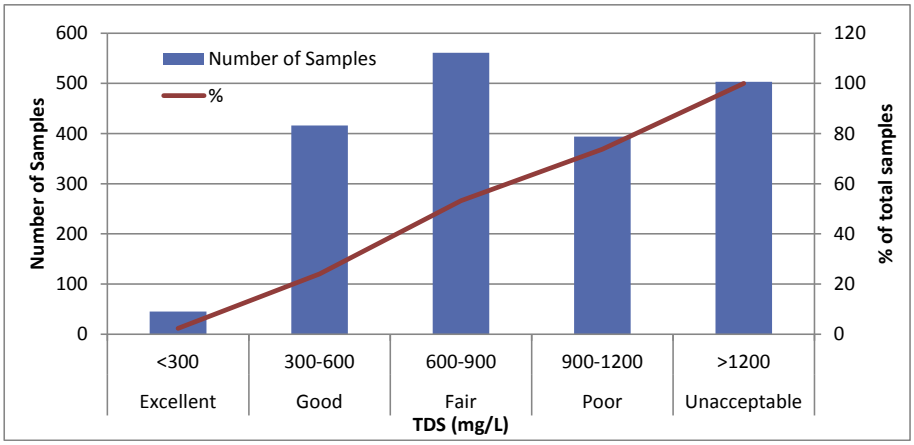

Fig. 27. Classification of historical groundwater quality samples data based on TDS WHO (2003).

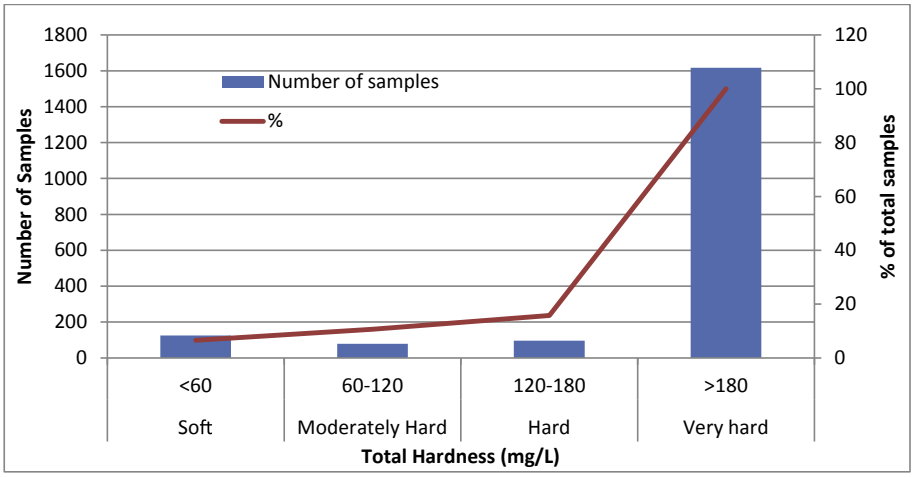

Fig. 28. Classification of groundwater Hardness (McGowan, 2000).

Bicarbonate Magnesium (HCO_3^- and Mg^{2+}) is the main hydrogeochemical type in the monitored groundwater system. This water type evolved from Acid Mine Drainage (AMD) buffering process. The AMD process occurring in the system is driven by the oxidation of pyrrhotite. The AMD is neutralized by carbonate minerals co-occurring with the acid-generating minerals. The elevated hardness in the majority of the groundwater samples is mainly due to the released of Mg^{2+} and Ca^{2+} ions into the system as result of AMD buffering process.

From the modelling results using PHREEQC it is found that Mg^{2+} and Ca^{2+} that evolve from carbonate AMD buffering process in the mine's groundwater system would only occur up to the certain points, where they would be limited. At these points their respective aqueous solubility will become limited by the saturation of calcite and dolomite. The neutralization of acid by carbonate minerals in the groundwater system has solved the pH problem but introduced a salinity problem.

Acknowledgments

We wish to acknowledge the Editor of the Journal of African Earth Sciences, and the reviewers of the present manuscript for their excellent work. We also acknowledge the University of the Free State for the postdoctoral fellowship.

References

Abid, K., Zouari, K., Dulinski, M., Chkir, N., Abidi, B., 2010. Hydrologic and geologic factors controlling groundwater geochemistry in the Turonian aquifer (southern Tunisia). Hydrogeol. J. 19, 415–427.
American Water Works Association and Water Environment Federation, 2005. Standard Methods for the Examination of Water and Wastewater. Washington, DC, pp. 20001–23710.
Armitage, P.E.B., McDonald, I., Edwards, S.J., Manby, G.M., 2002. Platinum-group element mineralization in the Platreef and calcsilicate footwall at Sandsloot, Potgietersrus district, South Africa. Appl Earth Sci. (Trans Inst Min Metall B) 111, B36–B45.
Bell, F.G., Bullock, S.E.T., Hälbich, T.F.J., Lindsay, P., 2001. Environmental impacts associated with an abandoned mine in the Witbank Coalfield. South Afr. Int. J. Coal Geol. 45, 195–216.
Belzile, N., Chen, Y.W., Cai, M.F., Li, Y., 2004. A review of pyrrhotite oxidation. J. Geochem. Explor. 84, 65–76.
Benner, S.,G., Gould, W.D., Blowes, D.W., 2000. Microbial populations associated with the generation and treatment of acid mine drainage. Chem. Geol. 169, 435–448.
Blowes, D.W., Ptacek, C.L., Frind, E.O., Johnson, R.H., Robertson, W.D., Molson, J.W., 1994. Acid-neutralization reactions in inactive mine tailings impoundments and their effect on the transport of dissolved metals. Proc. Int. Land Reclam. Mine Drain. Conf. Pitt. 1, 429–438.
Blowes, D.W., Ptacek, C.J., Jamvor, L.J., Weisener, C.G., 2003. The geochemistry of acid mine drainage. In: Holland, H.D., Turekian, K.K. (Eds.), Treatise on Geochemistry. Elsevier, New York, 9:149–204.
Buchanan, D.L., 1988. Platinum-group element exploration. In: Developments in Economic Geology, vol. 26. Elsevier, Amsterdam, pp. 73–76.
Burdon, D.J., Malzoum, J., 1958. Some chemical types of groundwater from Syria. In: Proceedings of the UNESCO Symposium, Teheran, pp. 73–90.
Bye, A.R., Bell, F.G., 2001. Stability assessment and slope design at Sandsloot open pit, South Africa. Int. J. Rock Mech. Min. Sci. 38, 449–466. PII: S 1 3 65-1 60 9 (0 1) 0 0 0 1 4 – 4.
Chizmeshya, A., McKelvy, M., Wolf, G., Carpenter, R., Gormley, D., 2003. Enhancing the atomic-level understanding of CO2 mineral sequestration mechanisms via advanced computational modeling. In: Tech. Rep. Arizona State University Center for Solid State Science.
Deutsch, W.J. (Ed.), 1997. Groundwater Geochemistry. Fundamentals and Applications to Contamination. Chemical Rubber Company (CRC) Press, Boca Raton.
Ekosse, G., Van Den Heever, D.J., De Jager, L., Totolo, O., 2004. Mineralogy of tailings dump around Selebi Phikwe nickel-copper plant, Botswana. J. Appl. Sci. Environ. Manag. 8 (1), 37–44.
Fey, M.V., 2010. Soils of South Africa. Cambridge University Press, Cape Town, 287 pp.
Fisher, R.S., Mulican III, W.F., 1997. Hydrochemical evolution of sodium-sulfate and sodium-chloride groundwater beneath the northern Chihuahuan desert, Trans-Pecos, Texas, USA. Hydrogeol. J. 10, 455–474.
Foose, M.P., Zientek, M.L., Klein, D.P., 1995. Magmatic sulfide deposits. In: du Bray, E.A. (Ed.), Preliminary Compilation of Descriptive Geoenvironmental Mineral Deposit Models, Open-File Report 95–831. U.S. Department of the Interior. U.S. Geological Survey.
Freeze, R.A., Cherry, J.A., 1979. Groundwater. Prentice Hall, New Jersey.
Geller, W., Friese, K., Herzsprung, P., Kringel, R., Schultze, M., 2000. Limnology of sulphur-acidic mining lakes. II Chemical properties: the main constituents and buffering systems. Verhandlungen Des. Int. Ver. Limnol. 27, 2475–2479.
Gomo, M., Vermeulen, D., 2014. Hydrogeochemical characteristics of a flooded underground coal mine groundwater system. J. Afr. Earth Sci. 92, 68–75.
Gomo, M., van Tonder, J.G., Steyl, G., 2012. Investigation of the hydrogeochemical processes in an alluvial channel aquifer located in a typical Karoo Basin of Southern Africa. Environ. Earth Sci. https://doi.org/10.1007/s12665-012-2118-9.
Guler, C., Thyne, G.D., McCray, J.E., Turner, A.K., 2002. Evaluation of graphical and multivariate statistical methods for classification of water chemistry data. Hydrogeol. J. 10, 455–474.
Guthrie, G.D., Carey, J.W., Bergfeld, D., Chipera, S., Ziock, H.-J., Lackner, K., 2001. Geochemical aspects of the carbonation of magnesium silicates in aqueous medium. In: NETL Meeting on Carbon Capture and Sequestration.
Henk, M. Haitjema, Sherry, Mitchell-Bruker, 2005. Are water tables a subdued replica of the topography? Ground water 43 (6), 781–786. https://doi.org/10.1111/j.1745-6584.2005.00090.x.
Holland, Martin, 2011. Hydrogeological Characterisation of Crystalline Basement Aquifers within the Limpopo Province, South Africa. PhD Thesis. University of Preotoria.
Jankowski, J., Beck, P., 2000. Aquifer heterogeneity: hydrogeological and hydrochemical properties of the Botany Sands aquifer and their impact on contaminant transport. Aust. J. Earth Sci. 47 (1), 45–64.
Jarvis, K., Carpenter, R., Windman, T., Kim, Y., Nunez, R., Alawneh, F., 2009. Reaction mechanisms for enhancing mineral sequestration of CO_2. Environ. Sci. Technol. 43 (16), 6314–6319.
Johnson, R.H., Blowes, D.W., Robertson, W.D., Jambor, J.L., 2000. The hydrogeochemistry of the Nickel Rim mine tailings impoundment, Sudbury, Ontario. J. Contam. Hydrol. 4, 49–80.
Lishman, Katherine Louise, 2009. The Acid Mine Drainage Potential of the Platreef, Nothern Limb of the Bushveld Complex, South Africa. A dissertation submitted to the Faculty of Science, University of the Witwatersrand, in fulfilment of the requirements for the degree of Master of Science, Johannesburg.
Kinnaird, J.A., McDonald, I., 2005. Mineralisation in the northern limb of the Bushveld complex. Appl. Earth Sci. (Trans. Inst. Min. Metall. B) 114, B194–B198.
Manyeruke, Tawanda D., Maier, Wolfgang D., Barnes, Sarah-Jane, 2005. Major and trace element geochemistry of the Platreef on the farm Townlands, northern Bushveld Complex. South Afr. J. Geol. 108, 381–396.
McDonald, Iain, Holwell, David A., Armitage, Paul E.B., 2005. Geochemistry and mineralogy of the Platreef and "Critical Zone" of the northern lobe of the Bushveld Complex, South Africa: implications for Bushveld stratigraphy and the development of PGE mineralisation. Miner. Deposita 40, 526–549. https://doi.org/10.1007/s00126-005-0018-6.
McGowan, W., 2000. Water Processing: Residential, Commercial, Light-industrial, third ed. Water Quality Association, Lisle, Illinois, USA.
Nordstroom, D.K., Alpers, C.N., 1999. Geochemistry of acid mine waters. In: Plumlee, G.S., Logston, M.D. (Eds.), The Environmental Geochemistry of Mineral Deposits: Part a. Processes, Methods, and Health Issues. Society of Economic Geologists, 6A. Reviews in Economic Geology, Littleton, CO, pp. 133–160.
Parkhurst, D.L., Appelo, C.A.J., 1999. PHREEQC for Windows Version 1.4.07. A Hydrogeochemical Transport Model. US Geological Survey Software.
Piper, A.M., 1944. A graphic procedure in the geochemical interpretation of water-analyses. In: Transactions, vol. 25. American Geophysical Union. https://doi.org/10.1029/TR025i006p00914 issn: 0002–8606.
Rose, A.W., Cravotta III, C.A., 1998. Geochemistry of coal mine drainage. In: Brady, K.B.C., Smith, M.W., Schueck, J. (Eds.), Coal Mine Drainage Prediction and Pollution in Pennsylvania. Bureau of Mining and Reclamation. Pennsylvania Department of Environmental Protection, Harrisburg.
SANS 241–1, 2015. Drinking Water, Part1: Microbiological, Physical, Aesthetic, and Chemical Determinants. The South African Bureau of Standards. ISBN 978-0-626-29841-8. Pretoria, South Africa.
Schwegler, Frank, 2003. Personal Communication. Geochemical Test Work to Evaluate Ore Stockpiles Z6/Z5 and Old Tailings Dam Disposal/retreatment Options. Anglo Platinum-PPL. Report No: CED/031/03.
Soil Classification Working Group, 1991. Soil Classification. A Taxonomic System for South Africa. Institute for Soil, Climate & Water, Pretoria.
Soregaroli, B.A., Lawrence, R.W., 1998. Update on waste rock characterization studies. In: Mine Design, Operations and Closure Conference, Polson, Montana.
Teir, S., Revitzer, H., Eloneva, S., Goelholm, C.-J., Zevenhoven, R., 2007. Dissolution of natural serpentine in mineral and organic acids. Int. J. Miner. Process. 83, 36–46.
Rian, Titus, Kai, Witthuser, Bruce, Walters, 2009. Groundwater and Mining in the Bushveld Complex. International Mine Water Conference 19th – 23rd October 2009. ISBN Number: 978-0-9802623-5-3 Pretoria, South Africa.
U.S. Environmental Protection Agency, 1996. Low Stress (Low Flow) Purging and Sampling Procedure for the Collection of Groundwater Samples from Monitoring Wells: Region 1 Low Stress (Low Flow) SOP, SOP # GW 0001, July 1996. Revision 2, 13 pp.
Vermeulen, D., Usher, B., 2009. Operation and monitoring guidelines and the development of a screening tool for irrigating with coal mine water in Mpumalanga Province, South Africa. Water SA 35 (4), 379–386.
Viljoen, M.J., Schürmann, L.W., 1998. Platinum-group metals. In: Wilson, M.G.C., Anhaeusser, C.R. (Eds.), The Mineral Resources of South Africa, vol. 16. Coun

Geosci Handbook, pp. 532–568.
Walton, W.C., 1962. Selected analytical methods for well and aquifer evaluation: Illinois State Water Survey, 49. Bulletin.
WHO, 2003. Total Dissolved Solids in Drinking-water. Background Document for Development of WHO Guidelines for Drinking-water Quality. WHO/SDE/WSH/03.04/16. Geneva, Switzerland.
WHO, 2011. Guidelines for Drinking-water Quality, fourth ed. ISBN 978 92 4154815 1. Geneva, Switzerland.